

Thermal Remote Sensing of Soil Moisture:

Validation of Presumed Linear Relation between Surface Temperature Gradient and Soil Moisture Content

by

Huang Qiu

A final year research project report submitted as part requirement for
subject 421-477

(Civil and Environmental Engineering Department)

at The University of Melbourne

November 2006

Supervisor: Jeffrey Walker
Co-supervisor: Clara Draper

Abstract

The thermal remote sensing technique provides a pathway to measure ground soil moisture (SM) content on the basis of the relationship between soil surface temperature and its moisture content using either thermal inertia or heat flux balance theories. Little work has been done towards the utilisation of surface temperature gradient (T_G) to infer subsurface soil moisture. Pegram (2006) proposed a hypothetical linear relationship between skin temperature gradient and top 5-cm soil moisture content. By computing the surface temperature gradient from thermal infrared (TIR) measurements by satellites, soil moisture content therefore can be retrieved by the relationship. This research aims to validate the presumed linear relation of soil moisture and surface temperature gradient, and to progressively explore optimum hourly period used to compute temperature gradients and the canopy effects on the relationship.

The known data set for this study contains surface temperature from thermal infrared spectrum and the in-situ soil moisture content (top 5cm) for a month long period over four different land surface types: *Illogan*(bare soil), *Stanley*(native grass), *Midlothian*(Lucerne crop) and *Merriwa Park*(wheat crop). Potential cloud influences on temperature gradient computations were excluded by classifying different cloud conditions (cloud-free, scattered and overcast) using incoming shortwave radiation data. Nine hourly periods were selected by eliminating the hourly periods around mid-day. Together with the four different vegetation covers, 36 scenarios were generated for evaluating the optimum hourly periods to be used in the relationship and the canopy effect.

Three criteria were proposed to evaluate the suitability of linear relation for each scenario: 1. wide temperature gradient range 2. high degree of linearity ($r^2 > 0.5$) and 3. least RMSE ($< 3\% v/v$). The first criteria is based on the fact that a larger T_G range could potentially reduce the sensitivity of T_G on soil moisture estimation, so that it avoids a small uncertainty in T_G to produce a large soil moisture estimation error. The second and the third criterion were based on statistical means to analyse the linearity of the relationship, they were utilised to ensure the maximum degree of linearity whilst producing the least estimating errors.

The analysis revealed two optimum scenarios: *Stanley* (1600-1700) and *Midlothian* (0900-1000). No optimum scenario was found at *Illogan* and *Merriwa Park*. Possible reason is that the soil moisture was not representative to their corresponding TIR sites. Nevertheless, the presence of the two optimum scenarios proves that the linear relationship can exist for some hourly periods on given canopy covers to a certain extent. Based on the findings of the study, instead of one optimum hourly period, the “best” hourly period to be used in the relationship could be flexible. Both morning and afternoon periods possess the ability to best describe the SM-TG relation, and the selection of best hourly period may be ultimately depending on the canopy cover, soil characteristics, topography and the latitude of the site. The analysis results of this study did not discover any clear relationship among the four study sites regarding the canopy effect. Hence, the no conclusion can be drawn regarding the canopy effect based on the results of this study.

Table of Content

ACKNOWLEDGEMENTS	IV
LIST OF ABBREVIATIONS	V
LIST OF FIGURES.....	VI
LIST OF TABLES	VIII
1. INTRODUCTION	1
2. BACKGROUND TO SOIL MOISTURE REMOTE SENSING	3
2.1 MICROWAVE REMOTE SENSING	3
2.1.1 <i>Passive Microwave Remote Sensing</i>	4
2.1.2 <i>Active Microwave Remote Sensing</i>	5
2.2 VISIBLE REMOTE SENSING	5
2.3 THERMAL INFRARED REMOTE SENSING	6
2.3.1 <i>Thermal Inertia (TI) Method</i>	7
2.3.2 <i>Heat Flux Balance Method</i>	7
2.3.3 <i>The Presumed TIR-SM Conversion Model by Pegram (2006)</i>	8
3. SITE AND DATA CHARACTERISTICS	11
3.1 STUDY AREA	11
3.2 DATA CHARACTERISTICS	13
3.2.1 <i>Soil Moisture Measurement</i>	15
3.2.2 <i>Soil Moisture Infilling</i>	16
3.2.3 <i>Representativeness of Ground Station Based Soil Moisture</i>	16
3.2.4 <i>Thermal Infrared Measurement</i>	17
3.2.5 <i>Surface Temperature Gradient T_G</i>	18
4. APPROACH AND ANALYSIS	22
4.1 SELECTION OF DESIRABLE HOURLY PERIODS	23
4.2 METHODS FOR SCENARIO EVALUATION.....	24
4.2.1 <i>Preliminary Screening</i>	24
4.2.2 <i>Temperature Gradient (T_G) Range</i>	27
4.2.3 <i>Statistical Analysis</i>	29
5. RESULT AND DISCUSSION	32
5.1 OPTIMUM SCENARIO	32
5.2 DISCUSSION.....	35
5.2.1 <i>Illogan and Merriwa Park</i>	35
5.2.2 <i>Midlothian and Stanley</i>	36
5.2.3 <i>Optimum Hourly Period</i>	37
5.2.4 <i>Canopy Effect</i>	37
6. CONCLUSION AND RECOMMENDATION	38
7. REFERENCES	40

Acknowledgements

This study was carried out thanking to the support of data from the: ‘National Airborne Field Experiment (NAFE)’ project. In particular, I am truly grateful to Jeffrey Walker, my project supervisor for his fruitful suggestions and all necessary assistances concerning every aspects of this research. He also offered me plentiful consultation time and provided me with independence. The research project could not have been completed without his timely supports.

I would also like to thank Clara Draper, my co-supervisor for her kindly assistance in reviewing my preliminary report and providing required data set and photographs. Thanks are also due to Rocco Panciera for his assistance in the data correction and provision.

List of Abbreviations

AET	Actual Evapotranspiration
ATI	Apparent Thermal Inertia
F _C	Field capacity of the soil in the sensing region [m ³ m ⁻³]
PET	Potential Evapotranspiration
SM	Volumetric Soil Moisture Content [m ³ m ⁻³]
SMSI	Soil Moisture Saturation Index
T _b	Brightness Temperature
T _G	Surface Temperature Gradient [°C/min]
T _{GL}	Lower limit of the temperature gradient [°C/min]
T _{GU}	Lower limit of the temperature gradient [°C/min]
TI	Thermal Inertia
TIR	Thermal Infrared
W _P	Wilting point of the soil in the sensing region [m ³ m ⁻³]

List of Figures

<i>Figure 1: Relating surface temperature to soil moisture conditions (Pegram,2006)</i>	9
<i>Figure 2a: SM-T_G relation with relatively large T_G range, T_G range=0.13</i>	10
<i>Figure 2b: SM-T_G relation with relatively small T_G range, T_G range=0.50</i>	10
<i>Figure 3. Map of the relative location of Goulburn River catchment in Australia</i>	11
<i>Figure 4. Map of the relative location of the four study sites in NSW, Australia</i>	11
<i>Figure 5a-d: Site characteristics of all sites</i>	12
<i>Figure 6a-d: Illustration of availability of all data at all sites</i>	14
<i>Figure 7. Schematic map of SM instrumental installation of study site. Although soil moisture were made at various depths, only the top 5cm SM data is concerned in this study.(Source: NAFE website)</i>	15
<i>Figure 8: Soil moisture infilling for Illogan. A sudden increase in SM on the graph suggests there was a rainfall event.</i>	16
<i>Figure 9. Schematic map of TIR instrumental installation of study site, showing soil temperature sensors at 1cm(T_1), 2.5cm(T_2) and 4cm (T_3) depths, leaf wetness sensor (L) and thermal infrared sensor (TIR). (Source: NAFE website)</i>	17
<i>Figure 10: Illustration of T_s gradient computation using the temperature measurements within an hourly period. Gradient unit: Deg(C)/minute.</i>	18
<i>Figure 11. Graph illustrating T_G change (to negative) for the hourly period where the cloud is present after 0830. The fitted trend-line has an r^2 of 0.5161.</i>	19
<i>Figure 12. Graph illustrates the soil surface temperature change become smaller due to the presence of cloud during the day.</i>	19
<i>Figure 13. Illustration of the cloud-free, overcast and scattered cloud days according to different cloud cover conditions. Data is extracted from the shortwave solar radiation collected from Stanley site.</i>	20
<i>Figure 14. The number of days that each hourly period is experiencing cloud-free (Class 1) condition.</i>	21
<i>Figure 15. The number of days that each hourly period is experiencing scattered cloud (Class 2) condition.</i>	21
<i>Figure 16. The number of days that each hourly period is experiencing overcast (Class 3) condition.</i> ..	21
<i>Figure 17: A schematic float chart outlines the procedures and methods for the study.</i>	22
<i>Figure 18. Plots of temperature gradient against each hourly period during the day. The red ellipses show the excluded periods around midday which have inconsistent gradients.</i>	24
<i>Figure 19a-d: Graphical representation of the SM-TG relation for all sites.</i>	25
<i>Figure 20a-d: Range of T_G and T_G deviations for each hourly period at all sites.</i>	28
<i>Figure 21: Graphical comparison of the relative magnitude of r^2 for all sites.</i>	29
<i>Figure 22: Graphical comparison of the relative magnitude of RMSE for all sites.</i>	31

Figure 23: $SM-T_G$ relationship for Stanley (1600-1700), the linear relationship is depicted by the equation $SM=-1.9357*T_G+0.4415$ 33

Figure 24: Comparison of estimated soil moisture and recorded soil moisture for Stanley (1500-1600).The gap between the first data point and second point illustrates the period of absent TIR data. 33

Figure 25: $SM-T_G$ relationship for Stanley (1600-1700), the linear relationship is depicted by the equation $SM=-1.0008*T_G+0.3461$ 34

Figure 26: Comparison of estimated soil moisture and recorded soil moisture for Midlothian (0900-1000). 34

Figure 27: r^2 and RMSE values for all hourly periods at Midlothian 36

Figure 28: r^2 and RMSE values for all hourly periods at Stanley 36

List of Tables

<i>Table 1: Summary of graphical interpretations for each site.....</i>	<i>26</i>
<i>Table 2: Summary of temperature gradient range for each site.....</i>	<i>27</i>
<i>Table 3: Scenarios with wide temperature gradient ranges.....</i>	<i>27</i>
<i>Table 4: Tabulation of r^2 for selected hourly periods for all study sites</i>	<i>29</i>
<i>Table 5: Scenarios with highest coefficient of determination r^2.....</i>	<i>30</i>
<i>Table 6: Tabulation of RMSE values for selected hourly periods for all study sites.....</i>	<i>30</i>
<i>Table 7: Scenarios with lowest root mean squared error (RMSE).....</i>	<i>31</i>
<i>Table 8: Summary of proposed scenarios based on the three criteria</i>	<i>32</i>
<i>Table 9: Optimum scenarios for the linear relationship</i>	<i>38</i>

1. Introduction

Soil moisture (SM) is considered as one of the most significant land environmental variables relative to land surface climatology, hydrology, and ecology. It defines the water content held in the soil generally within reach of plant roots and its spatial and temporal distribution has enormous implications in hydrological, agricultural, economic and social planning and development (Vicente *et al.* 2004). It is also worth clarifying that in this research, soil moisture is defined as the water content in the near surface portion of the soil, which is usually regarded as the soil moisture content over the top 5 cm of soil.

In both global and region hydrological cycles, soil moisture is also one of the key parameters linked to land surface evapotranspiration, runoff generation, surface infiltration and groundwater recharge. By observation and modelling the hydrological processes, the variation and impact of soil moisture can be obtained and relates to various practical applications. Some of these application examples are list as follows:

- The deviation between actual and desirable values of soil moisture is critical for the water resources management decision-making process;
- Forecasting of climate and weather variables: precipitation and temperature by estimating land-atmospheric water and heat (flux) transfer, respectively (Fast and McCorcle, 1991; Engman, 1992; Betts *et al.*, 1994; Su *et al.*, 1995);
- Flood predicting based on the spatial distribution of the saturation of ground soil (Entekhabi *et al.*, 1993; Su *et al.*,1995);
- Development of more efficient irrigation schedules/schemes from the knowledge spatial and temporal distribution of soil moisture;
- Rural and urban planning: pre-selection of plantation/crops based on soil moisture pattern/level to maximize the economic, environmental and social benefit;
- Investigating global climate change through persistence and change of high or low soil moisture content (Engman, 1992);
- Agricultural applications: estimate of grass growth by soil moisture;
- Other environmental and through hydrological modelling: erosion prediction (Western *et al.*, 1997), wetland maintenance and inland water body conservation.

However, accurate measurement of soil moisture is difficult because typical field methods, also known as point measurements, are both complex and expensive (i.e. labour intensive). Moreover, local scale variations in soil properties, terrain and vegetation cover make fully comprehensive assessment difficult in terms of selection of representative field sites and site access (Engman & Chauhan, 1997; Wood, 1997). Nevertheless, the recent advancing on remote sensing technology provides another pathway for the rapid areal and temporal estimate of soil moisture in ground near-surface zone.

Although a variety of remote sensing techniques is available for soil moisture retrieval depending on different electromagnetic spectrums being utilised, such as thermal infrared, microwave and visible spectrums, the preciseness of the prediction is ultimately determined by the model which relates the soil moisture and the remote sensing data.

Many models and algorithms have come in to being using difference remote sensing techniques. So far, none of those provide a simple and straightforward relationship between the observed remote sensing data and the actual soil moisture. Most of these methods require complex empirical modelling processes and are dependent on a variety of parameters which are difficult to measure and acquire due to their large variability. A thermal infrared technique proposed by Pegram (2006) based

on a linear relationship between average soil moisture (SM) and surface temperature gradient (T_G) suggests a relative simple method in retrieving near-surface soil moisture.

The basis for Pegram's TIR-SM conversion model is the strong dependence of the thermal properties of soil and water on surface temperature change. With the established knowledge of temperature - thermal properties- soil moisture relations, it is shown that the temperature gradient on a particular area (or called as a pixel on a large remote sensing image) for a fixed period of time would in some way be inversely related to the average soil moisture content over the area (Pegram, 2006). As such, by calculating the surface temperature gradients from remote sensed thermal infrared data, the near-surface soil moisture can be estimated from the relationship.

In order to test and verify this relationship, a month long thermal infrared and soil moisture data in four study sites of different vegetation covers in the Goulburn River catchment will be utilised in this research. The four different vegetation covers include: bare soil, native grass, Lucerne crop and wheat crop, which was present in *Illogan*, *Stanly*, *Midlothian* and *Merriwa Park*, respectively. The thermal infrared data was obtained by using thermal infrared spectrum from ground station sensors installed in the four study sites every 5 minutes, whilst the in situ soil moisture was measured by the Hydraprobe at 20-minute interval.

With the measured surface temperature and soil moisture data, the presumed linear relationship between skin temperature gradients and soil moisture is tested using this data set for selected hourly intervals from 0700 to 2000 each day for one month's period, so as to determine the most appropriate temporal interval to be used in the model. The appropriateness of an hourly period is based on three criteria: the range of surface temperature gradient, the linearity of the relationship (r^2) and the potential estimation errors (RMSE). Evaluation of the range of T_G is designated to minimize the possible SM estimation error caused by the uncertainty of temperature gradient, whereas the evaluation of linearity and potential error is to verify the fundamental applicability of the SM/ T_G relationship. As well as hourly period, the influences of different vegetation covers on the presumed relationship are also evaluated.

It should be noticed that no seasonal effect is taken into account for the study because only month long data sets are being used in the study. This research was carried out to verify the applicability of the presumed SM/ T_G relationship on a regional basis. Therefore, results of this research only reflect the regional appropriateness of the proposed relationship in the specific period during which the data were taken and utilised.

2. Background to Soil Moisture Remote Sensing

Typical remote sensing techniques for soil moisture estimation involve the collection and interpretation of satellite imaging, aerial photography or ground monitoring station data regarding the nature, properties and state of the soil. These variations and differences of the soil nature, properties and state are reflected and picked by the sensors installed on the satellites depending on their different electromagnetic spectrum properties. Currently, a variety of remote sensing techniques for soil moisture retrieval has been evolving based on their different electromagnetic spectrum properties. Given measured ground/atmospheric data by the remote sensing system and the existing theories, a certain number of models have been developed by researchers to retrieve the unknown soil moisture both spatially and temporally. Four major prevailing SM remote sensing techniques based on the spectrum properties are summarized as follows (Vicente *et al.*, 2004; Walker, 1999)

- Passive microwave: calculate SM by measuring brightness temperature (T_b), determination of soil dielectric properties and soil temperature
- Active microwave (SAR): calculate SM based on backscatter coefficient and dielectric properties
- Visible: calculate SM by based on soil albedo index of refraction
- Thermal infrared: calculate SM by measuring soil surface temperature

2.1 Microwave Remote Sensing

Although many previous research has shown that several remote sensing techniques can be used to estimate surface soil moisture, microwave systems appear to be the best suited to potential remote sensing applications because they provide a direct estimate of soil moisture and weather independent (Jackson, 1984). Operational microwave technologies from remote platforms have wavelengths in the range of a few centimeters to a few decimeters ~C, L, P bands are equivalent to wavelength of 5.6, 21, and 68 cm or frequency of 5.3, 1.4, 0.438 GHz, respectively (Scott *et al.*, 2003).

Microwave remote sensing can be categorized into two types depending on their source of electromagnetic energy: active and passive microwave. As the name suggests, active microwave technique has its own source of electromagnetic radiation to measure the energy that is reflected and scattered back from its origin, radar is a typical example of this type. In contrast, passive microwave measures the natural electromagnetic spectrum emitted from the soil, hence no additional aid of external electromagnetic energy is required.

The principle underlying both passive and active microwave sensing of soil moisture is the large contrast of dielectric properties of water content and dry soil. Dielectric properties can be plainly defined as the resistance of a substance to electric current. It is commonly expressed using the relative term “dielectric constant”, which consists of real (ϵ') and imaginary parts (ϵ'') by the relationship as follows:

$$\epsilon = \epsilon' - \epsilon'' \quad (1)$$

Based on the knowledge of the dielectric properties of the soil medium, it is known that the contrast between the dielectric constant of water and that of dry soil is larger. With different dielectric

constant in soil medium, the propagation characteristics of an electromagnetic field within that medium are also varying. Consequentially, the spectral emissions from the soil particles, air and water within the soil medium is affected by the different dielectric constant when they passes through it (Walker, 1999). By measuring the strength of the spectrum, the proportion of water in the soil can be clearly manifested through the dielectric properties.

Some existing dielectric models that relate dielectric properties and the moisture of soil include the model of Wang and Schmugge (1980), Dobson *et al.* (1985) and Peplinski *et al.* (1995). Among which, Peplinsk Dielectric mixing model is the most widely and commonly used theory, considering being a compromise between the complexity of the theoretical models and the simplicity of the empirical models (Walker *et al.*, 2004a).

2.1.1 Passive Microwave Remote Sensing

Passive microwave makes use of a microwave radiometer (or sensor) which measures the energy that is radiated (by thermal emission) or reflected (from the sun or other radiating objects) by the earth's surface or atmosphere (Woodhouse, 2005). The intensity of the energy measured is characterised by the Brightness Temperature (T_b), which is dependent on the soil dielectric properties and the soil temperature at the measured point.

The fundamental of passive microwave remote sensing relies on the fact that the emissivity (e) at microwave wavelengths is a function of the dielectric constant of the soil-water mixture and thus the soil moisture. The variation in soil emissivity in microwave region is relatively weak, with a range from ~0.95 for dry soil and ~0.6 or less for wet soil (Walker, 1999) and it is affected by a number of factors: such as soil texture, surface roughness and vegetation cover. The texture affects the slope of the relation between e and soil moisture but not the range of variation. Roughening of the soil surface increases soil emissivity and decreases the sensitivity to soil moisture content, thus reducing the range of brightness temperature from wet to dry soils (Van de Griend and Engman, 1985). Vegetation cover also reduced the variation of emissivity in a way that the canopy can absorb some of the radiation coming up from the soil and emitting radiation itself (Walker, 1999). While both roughness and vegetation affect the range of variation, vegetation is more significant because it can totally obscure the soil surface if it is present in sufficiently large amounts.

Passive microwave sensors are typically radiometers or scanners, such as Electrically Scanning Microwave Radiometer (ESMR), Scanning Multichannel Microwave Radiometer (SMMR), Special Sensor Microwave/Imager (SSM/I) sensors and newest Advanced Microwave Scanning Radiometer–Earth Observing System (AMSR-E) sensors. The microwave energy recorded by a passive sensor can be emitted by (1) the atmosphere, (2) reflected from the surface, (3) emitted from the surface, or (4) transmitted from the subsurface. Because the wavelengths are relatively long, the energy available is quite small compared to optical wavelengths. Thus, the measurable fields must be large to detect enough energy to record a signal. Most passive microwave sensors are therefore characterized by low spatial resolution, which is also regarded as one of the major limitation of passive microwave remote sensing. Nevertheless, generally speaking, as the long wavelength, passive microwave sensing is less vulnerable to the atmospheric noise, such as cloud covers and rains. It also possesses greater vegetation penetration ability than other spectrums. Another major limitation for the utilisation of passive microwave technique is the absence of a dedicated soil moisture satellite with the L-band spectrum (considered the optimum band for soil moisture retrieving applications). However, it is believed that with the launch of European HYDRO/SMOS satellite, the use of passive microwave can be enormously enhanced.

2.1.2 Active Microwave Remote Sensing

Active microwave technique uses active sensors, such as radar systems, to generate their own illumination by transmitting pulses of microwave radiation and then measure the scattered signal from the area of interest by receiver systems (Woodhouse, 2005). One most common imaging active microwave configuration is the synthetic aperture radar (SAR), which transmits a series of pulses as the radar antenna traverses the scene. Then, these pulses are processed together to simulate a very long aperture capable of high surface resolution (Ulaby *et al.*, 1996).

The scattered signal is the key for the soil moisture retrieval using active microwave. Intensity of scattered signal of earth's surface is governed by its geometrical and dielectric properties relative to the incident radiation, the variations in backscattering are influenced by soil moisture content, surface roughness, surface cover (vegetation), topography, observation frequency, wave polarisation and incidence angle (Walker *et al.*, 2004a).

A variation of relative dielectric constant between 3 and 30 (a shift in volumetric moisture content between approximately 2.5% and 50%, depending on frequency and soil texture) will cause an 8 to 9 dB rise in backscatter coefficient for vv (vertical transmit vertical receive) polarization (Hoeben *et al.*, 1997, Walker *et al.*, 2004a). It is this relationship between backscattering coefficient and dielectric constant enables the retrieval of soil moisture.

Several models have been developed to describe the connection between dielectric properties and backscatter coefficient, offering a number of ways for soil moisture computation. Some common models are listed as below:

- The empirical model (EM) of Oh *et al.* (1992);
- The theoretical integral equation model (IEM) of Fung *et al.* (1992); and
- The semi-empirical model (SEM) of Oh *et al.* (1994).

In summary, the soil moisture retrieval using active microwave is depending on an active source of energy transmitting to determine the intensity of backscattered signal, and the relationships between backscatter coefficient, dielectric constant and soil moisture.

Despite a variety of models exists for soil moisture computation using active microwave, the active microwave technique is very much limited by its high sensitivity to surface roughness, topographic features and vegetation cover than passive microwave system, which give certain difficulties in the moisture-backscatter coefficient inversions. But in applications requiring high spatial resolution, active microwave is still superior over the passive system.

2.2 Visible Remote Sensing

The visible regions of the electromagnetic spectrum have been the most commonly used in remote sensing of planetary surfaces due to the fact that this spectral region of maximum illumination by the sun and most widely available detectors (Elachi, 2006). The visible remote sensing of soil moisture depends on the measurement of the reflected radiation (i.e. albedo) of the sun from the earth's surfac. Using the known relationship between albedo and soil moisture, soil moisture can be obtained. However, in soil moisture retrieval applications, visible sensing technique is rarely used owing to the following reasons:

1. The reflected radiation can be easily influenced by many factors, such as organic matter, soil texture, surface roughness, angle of incidence, plant cover and color (Engman, 1991; de Troch *et al.*, 1996; Walker, 1999), causing large variation in albedo of different soil types (Sadeghi *et al.*, 1984). Hence, it does not give high accuracy and precision in soil moisture computation.
2. As shown by many research, the detectable depth of moisture of soil is proportional to the wavelength utilised in remote sensing technique. The visible region of the electromagnetic spectrum only enables the detection of the top few millimeters of the soil profile.

2.3 Thermal Infrared Remote Sensing

Objects that have a temperature above absolute zero (0 K) emit electromagnetic energy at all wavelength. Therefore, all the features in landscape (i.e. vegetation, soil, animals, water) emit thermal infrared electromagnetic radiation in the 3.0 – 14 μm portion of the spectrum (Jensen, 2006). The potential for the estimation of soil moisture is based on the excellent thermal emission ability of earth surface.

There are distinct differences between the thermal properties of soil and water, including Heat Capacity (C), Thermal Conductivity (K) and Thermal Inertia (P). Therefore, a little change of the soil-water portion gives a large change in the thermals properties. By detecting the thermal properties of the ground, the soil moisture can then be obtained by applying the established models or methods. Because the detectable radiation emitted by the earth's surface not solely depends on the surface temperature, but also the soil surface emissivity, so the emissivity has to be assumed or empirically determined when applying the models.

Apart from emissivity, several external factors are also to be taken into account when using thermal infrared technique. As thermal region of electromagnetic spectrum has low penetrating ability, atmospheric effects are considered as some large impediments. Furthermore, ground vegetation also prevents the thermal spectrum to pass through. If the vegetation cover consists of dense canopy, and obscures more than about 10 to 20% of the soil surface, then the resulting image produced by the thermal remote sensor may have no relation to the radiation temperature of the earth's surface below. If the vegetation cover is predominantly low grass, then the resulting image is closely related to the earth's surface temperature (Pratt and Ellyett, 1979). There, if the vegetation cover is significant over the targeting region, instead of measuring the soil surface thermal properties, the thermal properties of vegetation would be acquired. Regions with little vegetation (i.e. bare soil) will be preferable for the thermal infrared remote sensing.

In addition to the vegetation factor, thermal approaches have some other drawbacks such as limited surface penetration depth, high perturbation of the signal by clouds and bushfires and signal attenuation by the earth's atmosphere. A series of complex noise removal mechanisms are often to be employed before the utilisation of the thermal data. Nevertheless, the capacities for higher spatial resolution, broad coverage, multi-satellite sensor availability, high and regular revisit frequencies, the possibility for real-time applications and the strong relationship between surface soil moisture content and temperature are however very promising (Verstraeten, 2006).

So far, researchers using thermal infrared data for soil moisture retrieval prevalingly focus on the thermal inertia related theory (Jordon and Shih, 1993; Ottl' and Vida-Madjar, 1994; Pratt and Ellyett, 1979; Verstraeten, 2006).and the theory associated with heat fluxes transfer in energy balance (Monteith 1981; Ben-Asher *et al.*, 1983), which are introduced as follows.

2.3.1 Thermal Inertia (TI) Method

This method is based on the fact that water bodies have a higher thermal inertia (TI) than dry soils and rocks and exhibit a lower diurnal temperature fluctuation. When soil water content increases, thermal inertia proportionally increases as well, thereby reducing the diurnal temperature fluctuation range. TI can be derived, starting from the temperature diffusion equation.

Several models have been developed using the thermal inertia method by Xue and Cracknell (1995), Sobrino and El Kharraz (1999) and Mitra and Majumdar (2004) for soil moisture retrieval based on the above mentioned principle but with slightly different approaches. Among which, Mitra and Majumdar (2004)'s approach is considered as the most direct method and analogous to the presumed model by Pegram (2006).

In their approach, apparent thermal inertia (ATI, assumed homogeneous layer for TI) is used. ATI is inferred by the measurements of spectral surface albedo and the diurnal temperature range. It represents the temporal and spatial variability of soil and canopy moisture (Tramutoli *et al.*, 2000). The higher ATI, the higher the moisture content of the surface. The fundamental to derive soil water content is based on the fact that high/low ATI values correspond to maximum/minimum soil moisture contents (Verstraeten, 2006). By incorporating the soil moisture saturation index, the model is described by the following relationships:

$$\text{SMSI}(t) = \frac{\theta(t) - \theta_{\text{res}}}{\theta_{\text{sat}} - \theta_{\text{res}}} \quad (2)$$

$$\text{SMSI}_0(t) = \frac{\text{ATI}(t) - \text{ATI}_{\text{min}}}{\text{ATI}_{\text{max}} - \text{ATI}_{\text{min}}} \quad (3)$$

$$\theta(t) = \text{SMSI}_0(t) \cdot (\theta_{\text{sat}} - \theta_{\text{res}}) + \theta_{\text{res}} \quad (4)$$

In equation (2), (3) and (4):

$\text{SMSI}(t)$	is the moisture saturation index at a time t [-];
$\text{SMSI}_0(t)$	is the remotely sensed topsoil moisture saturation index [-];
$\theta(t)$	is volumetric soil moisture content at a time t [$\text{m}^3 \text{m}^{-3}$];
$\theta(\text{res})$	is volumetric residual soil moisture content [$\text{m}^3 \text{m}^{-3}$];
$\theta(\text{sat})$	is volumetric saturated soil moisture content [$\text{m}^3 \text{m}^{-3}$];
$\text{ATI}(t)$	is the apparent thermal inertia at time t [K^{-1}];
ATI_{min}	is the minimum apparent thermal inertia [K^{-1}];
ATI_{max}	is the maximum apparent thermal inertia [K^{-1}];

2.3.2 Heat Flux Balance Method

This method of retrieving soil moisture in the thermal infrared range was done earlier by Idso *et al.* (1975), Reginato *et al.* (1976) and Price (1980). The theory is based on the relationship with energy

balance that expressed the partition of latent and sensible heat fluxes (Sellers 1965, Monteith 1981, Ben-Asher *et al.* 1983) to infer soil moisture content:

$$Q=G+H+L \quad (5)$$

where G, H and L are fluxes (Wm^{-2}) of soil heat, sensible heat, and latent heat, respectively.

One of the techniques which makes use of this theory is called the surface energy balance algorithm for Land (SEBAL), which is an image-processing model comprised of 25 computational steps that calculates the actual and potential evapotranspiration (PET) and other energy exchanges at the earth's surface using digital image data collected by Landsat or other remote-sensing satellites (Scott *et al.*, 2003). A complete radiation and energy balance for the surface along with heat fluxes and resistances for momentum, heat and water vapour transport is computed from the SEBAL. Evapotranspiration is then computed as a component of the energy balance on a pixel-by-pixel basis. Whereas actual evapotranspiration (AET) is based on an energy balance residual term, potential evapotranspiration (PET) is based on a minimum surface resistance that is a function of leaf area index and reduction terms for ambient heat and water vapour stress (Scott *et al.*, 2003). After this step, approximation of volumetric soil moisture is obtained using an established statistical relationship between moisture and the evaporative fraction of latent heat.

2.3.3 The Presumed TIR-SM Conversion Model by Pegram (2006)

Although many models and algorithms have come in to being using the aforementioned means, none of those provide a simple and straightforward relationship between the observed remote sensing data and the actual soil moisture. Most of these methods require complex empirical modelling processes and are dependent on a variety of parameters, which are difficult to measure and acquire due to their large variability. A thermal infrared technique developed by Pegram (2006) based on a linear relationship between average soil moisture (SM) and surface temperature (ST) gradient suggests a relative simple method in retrieving near-surface soil moisture.

The basis for Pegram's thermal infrared-soil moisture conversion model is the strong dependence of the thermal properties of soil and water (i.e. heat capacity (C), thermal conductivity (K) and thermal inertia (P)) on surface temperature change. With the established knowledge of temperature - thermal properties- soil moisture relations, past research has shown that the temperature gradient on a particular area (otherwise known as a pixel on a large remote sensing image) for a fixed period of time would in some way be inversely related to the average soil moisture content over the area (Pegram, 2006). As such, by calculating the surface temperature gradients from remote sensed thermal infrared data, the near-surface soil moisture can be estimated from the relationship.

The temperature change (i.e. gradient) is thus assumed solely affected by the soil moisture, where other factors such as wind (i.e. might accelerated the evaporation) is not taken into account. The theory and procedures behind this method is thought as analogous to Mitra and Majumdar (2004)'s Thermal Inertia methods. Procedures of the Pegram (2006)'s method are summarized as follows:

1. The conversion of satellite (i.e. METEOSAT-8) measured brightness temperature (thermal infrared data) to the surface temperature by split window algorithm.
2. The five estimated surface temperatures (T_s) on each pixel for each day between 0800 and 0900 local time at 15 minute intervals were extracted from the archive and used to calculate the temperature gradient.

3. Atmospheric correction by refining temperature gradient data pool using statistical method (i.e. normal distribution of the slope and coefficient of determination r^2) to eliminate inconsistent data. The inconsistent data is usually caused by the cloud cover and grass fire. After correction procedures, highest and lowest temperature gradients are selected from the data pool.
4. Obtain known *wilting point* and *field capacity* of the study sites. A steep temperature gradient is expected for drier soils and the converse for wet soil, so the highest recorded temperature gradient can be said to correspond to the drier of the known *wilting point*. The converse can be also said to hold true for *field capacity*.
5. The relation between soil moisture θ and the temperature gradient T_G for a given soil type is given the expression as follows and relationship in *Figure 1*:

$$\theta = \frac{F_C - W_P}{T_{GL} - T_{GU}} \cdot T_G + C \quad (6)$$

In equation (6):

θ	is predicted volumetric soil moisture content [$m^3 m^{-3}$];
F_C	is field capacity of the soil in the sensing region [$m^3 m^{-3}$];
W_P	is wilting point of the soil in the sensing region [$m^3 m^{-3}$];
T_{GL}	Lower limit of the temperature gradient [$^{\circ}C/min$];
T_{GU}	Upper limit of the temperature gradient [$^{\circ}C/min$];
T_G	Surface temperature gradient [$^{\circ}C/min$];
C	Constant [$m^3 m^{-3}$].

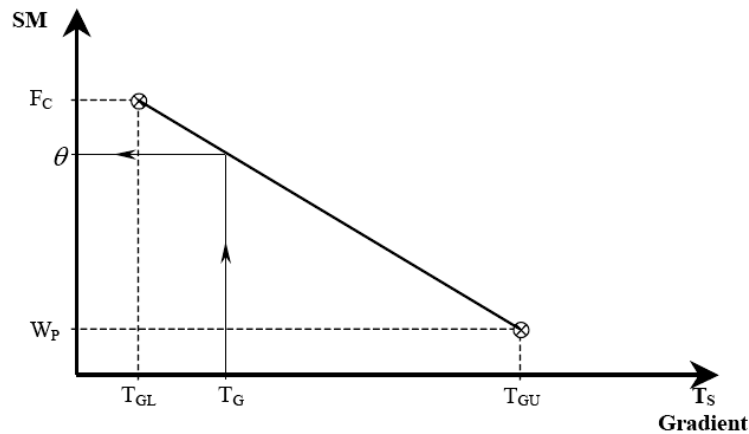


Figure 1: Relating surface temperature to soil moisture conditions (Pegram,2006)

6. Apply T_G into the prescribed relationship above to infer soil moisture for different time during the year.

According to this methodology, the hourly surface temperature gradient is taken from 0800 to 0900 in the mornings every day (from remote sensing perspective, early morning periods are most likely to be cloud free compared to other hourly periods of the day, so it is deemed more appropriate for remote sensing applications) and the linearity of the relationship is assumed to be linear. However, this gives rise to three questionable points:

1. Linearity of the relationship, which is also the core of the Pegram's proposal.

- Whether 0800-0900 is the best hourly period that describes this relationship. This is because the different parts of the earth receive different solar radiation, hence, for a fixed hourly period, the temperature gradients might vary from one place to another. It is likely that other hourly periods could give a better linearity of the relationship.

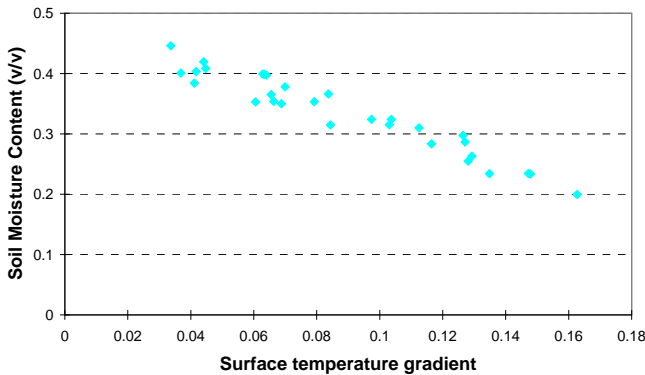


Figure 2a: SM- T_G relation with relatively large T_G range, T_G range=0.13

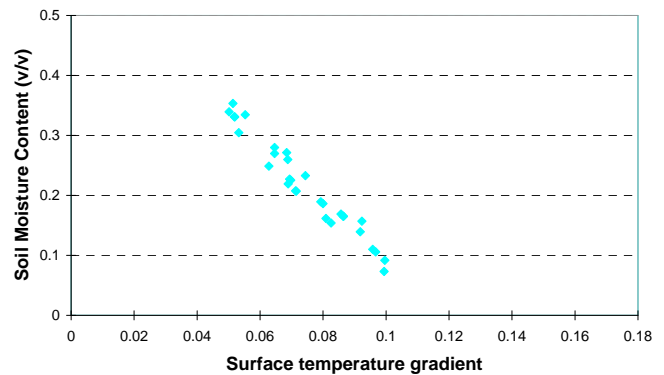


Figure 2b: SM- T_G relation with relative small T_G range, T_G range=0.05.

- Provided the relationship was linear, the range of T_G correlating to the soil moisture is also crucial. The term ‘range’ here is referring to the maximum and minimum T_G value for a relationship, which correspond to the driest soil and wettest soil respectively. A small range of T_G may give large errors in soil moisture estimation because a slight uncertainty in gradient value will lead to large soil moisture difference. *Figure 2a-b* above illustrate the importance of the T_G range in the relationship. It can be seen that if an uncertainty occurs (say 0.01 °C/min) in temperature gradient, relationship in *Figure 2a* gives ~3% v/v possible error in soil moisture estimation, whereas *Figure 2b* leads to ~8% v/v errors.
- Canopy impact is not mentioned in Pegram’s methodology; however, in the context of this study, the extent of impact of surface vegetation on the relationship will be investigated.

It is these four points that raises the initiatives of this study to verify this methodology and to seek for likely improvements. In the research, the hourly period will not only be confined in 0800-0900, but further elaborated for other possible hourly periods during the day, in the hopes that an alternative hourly period which best describes the linearity and possessing large T_G range could be found.

As stated by many researchers, canopy density has significant impact on the surface temperature measurement by thermal infrared spectrum but this has not yet been discussed in Pegram’s methodology. Nemani *et al.* (1993) pointed out that different fractional vegetation cover would affect the measured thermal temperature. For example, in fully vegetated areas, thermal changes maybe associated with changes in the green cover evapotranspiration, which is eventually conditioned by soil moisture content. Therefore, the influence of the vegetation cover on the relationship will be investigated based on the four different vegetation covers included in the study. These four vegetation covers are bare soil, native grass, Lucerne crop and wheat crop, ordered with increasing vegetation density.

3. Site and Data Characteristics

3.1 Study Area

The data used in this research is collected from four different experimental sites in the Goulburn River catchment (*Figure 3*) during November 2005, each with a distinct vegetation cover type, including bare soil, native grass, Lucerne crop and wheat crop. The four study sites are selected from several experimental sites of The National Airborne Field Experiments (NAFE), which was designed for a variety of remote sensing and soil moisture related studies.

The Goulburn River catchment is located within the semi-arid region approximately 200km west of Newcastle, on the east coast of Australia. The northern half of this catchment has predominantly low to moderate vegetation cover and is used for cropping and grazing, while the southern half of the catchment is more heavily vegetated, including a National Park. Soils in the northern section are predominately basalt derivatives while those in the south are sandstone derivatives (SASMAS, 2003).



Figure 3. Map of the relative location of Goulburn River catchment in Australia

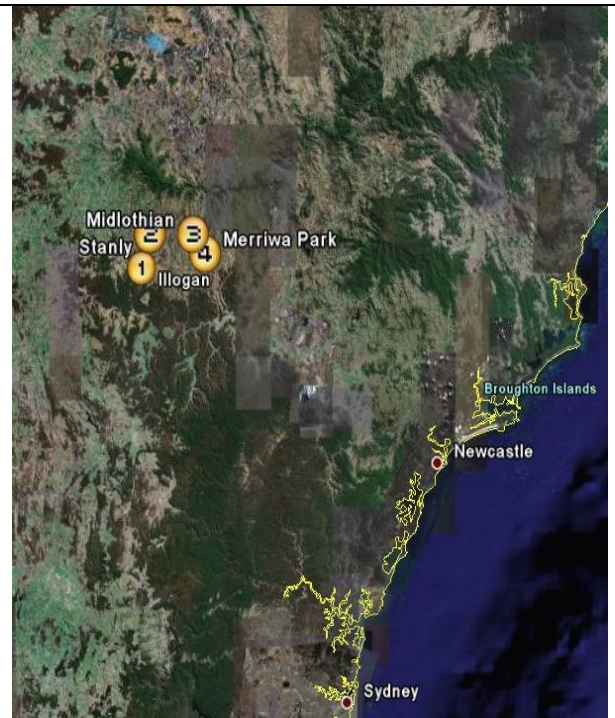


Figure 4. Map of the relative location of the four study sites in NSW, Australia

The four study sites shown in *Figure 4* are characterised by four different vegetation cover (from vegetation scarcity to vegetation abundance): Bare Soil (i.e. no vegetation), Native Grass, Lucerne Crop and Wheat Crop for Illogan, Stanley, Midlothian and Merriwa Park, respectively. Clay is the predominant soil type in all the study sites. Details of each site are provided on next page:

1. Illogan



Site characteristics

Longitude	150° 4' 36"E
Latitude	32° 9' 19"S
Elevation	360m
Slope	2.8°
Aspect	95°
Soil depth	70cm
Soil type	Clay Loam
Vegetation type	Bare soil

Figure 5a: Site characteristics of Illogan

2. Stanley



Site characteristics

Longitude	150° 7' 27"E
Latitude	32° 5' 31"S
Elevation	329m
Slope	2°
Aspect	284°
Soil depth	>90cm
Soil type	Clay
Vegetation type	Native grass

Figure 5b: Site characteristics of Stanley.

3. Midlothian



Site characteristics

Longitude	150° 21' 46"E
Latitude	32° 01' 16"S
Elevation	311m
Slope	<1°
Aspect	152°
Soil depth	60-90cm
Soil type	Clay
Vegetation type	Lucerne crop

Figure 5c. Site characteristics of Midlothian.

4. Merriwa Park



Site characteristics

Longitude	150° 25' 50"E
Latitude	32° 05' 55"S
Elevation	417m
Slope	2°
Aspect	107°
Soil depth	60-90cm
Soil type	Clay
Vegetation type	Wheat crop

Figure 5d. Site characteristics of Merriwa Park.

The photographs and site information in Figure 5a-d are referring to the thermal infrared stations and used for illustration purpose only.

3.2 Data Characteristics

Two types of data are to be used in the study, they are: thermal infrared data and top 5cm soil moisture data. The thermal and soil moisture data were obtained from in situ measurements using the Thermal infrared (Everest Interscience Inc.?) and soil moisture sensors (Stevens Water Hydraprobe), respectively. Except for *Stanley*, thermal infrared and soil moisture measurements were not made in exactly the same position in each study site but with different ground stations within a close distance (less than 1km). And this fact is regarded as one of the major assumptions in the study, that is, the SM and TIR data are mutually compatible to use to test the presumed relationship.

Nevertheless, for the sites at which SM and TIR measurements were made in different location, a certain number of separate hand measurements of SM which made at a closer distance from the TIR station are available to assess how representative of the ground station based soil moistures to the TIR sites. These hand SM measurements were made within 300m of the vicinity of the TIR station and were thought to be approximately equivalent to the soil moisture of the TIR station site.

The thermal infrared data was obtained from the TIR sensors installed at each monitoring station. TIR data is firstly to be converted to hourly temperature gradient (with respect to time) for the whole length of the period when data was taken. After this conversion, with the aid of shortwave radiation data, the data will be trimmed to eliminate the cloud influence on the temperature gradient computation.

An overview of data availability is shown in *Figure 6a-d* next page for all study sites. It is noticeable that there is no hand measurements were made at *Stanley* as SM and TIR measurements were located at the same postion. The soil moisture (top 5cm) data at *Illogan* shown in *Figure 6a* is the complete data set after SM data infilling. Infilling process is detailed in Section 3.2.2.

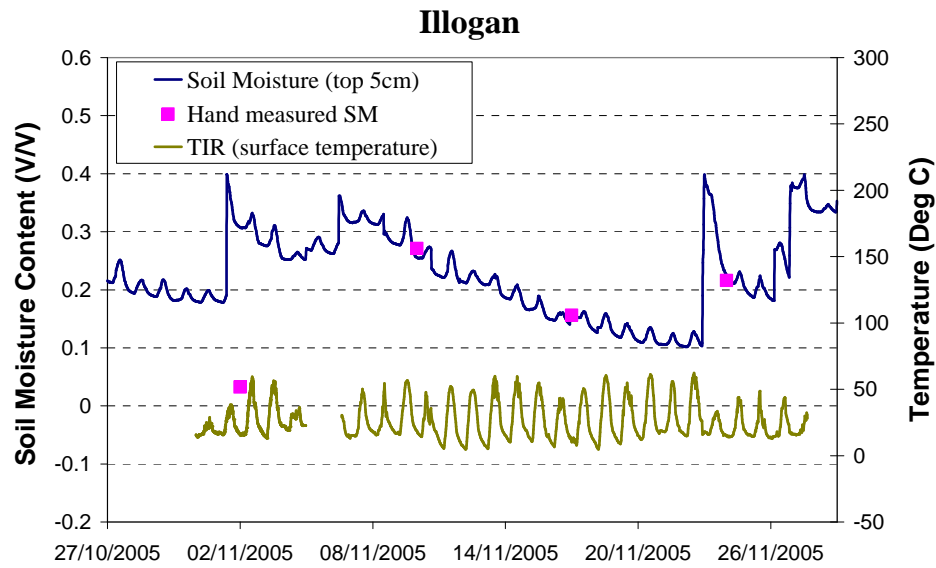


Figure 6a: Illustration of availability of all data at Illogan

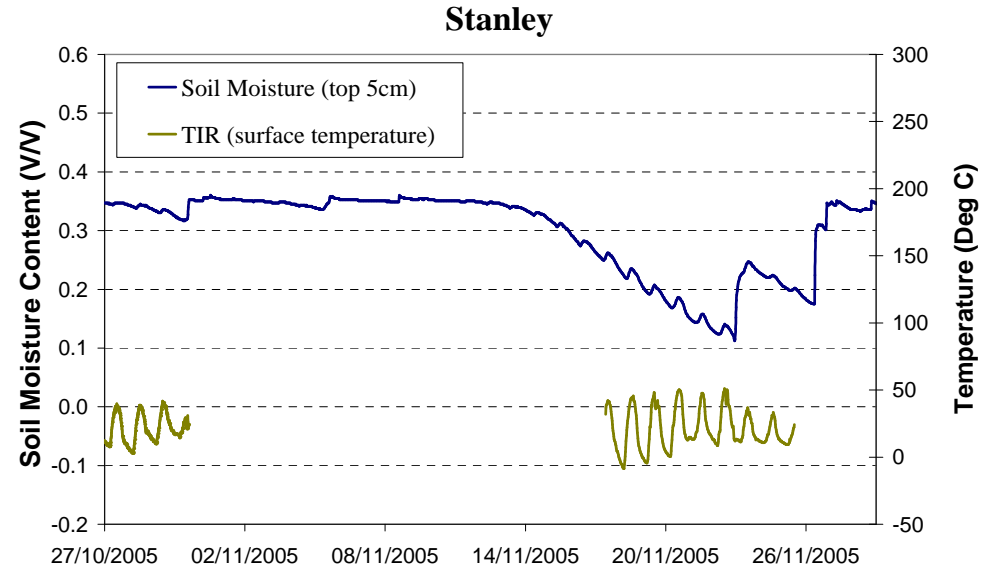


Figure 6b: Illustration of availability of all data at Stanley

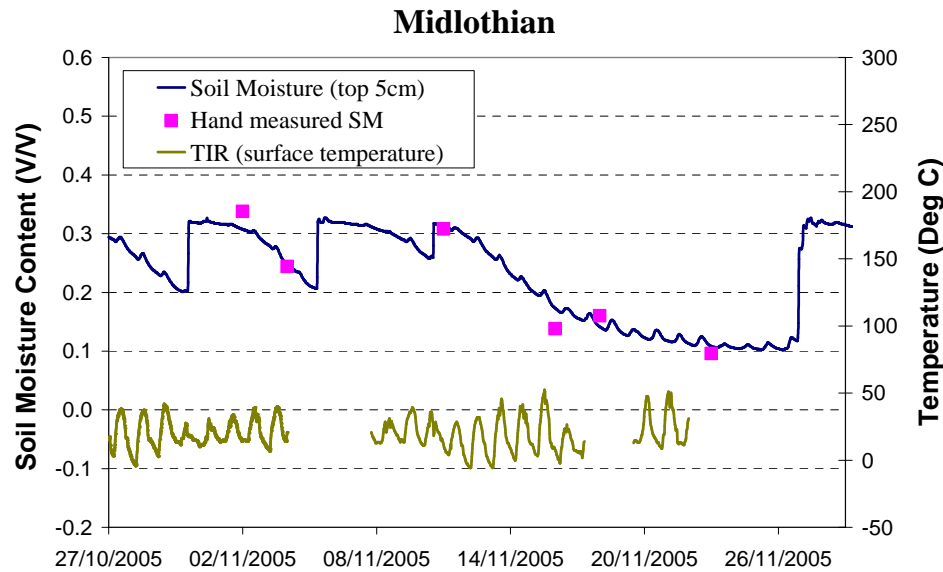


Figure 6c: Illustration of availability of all data at Midlothian

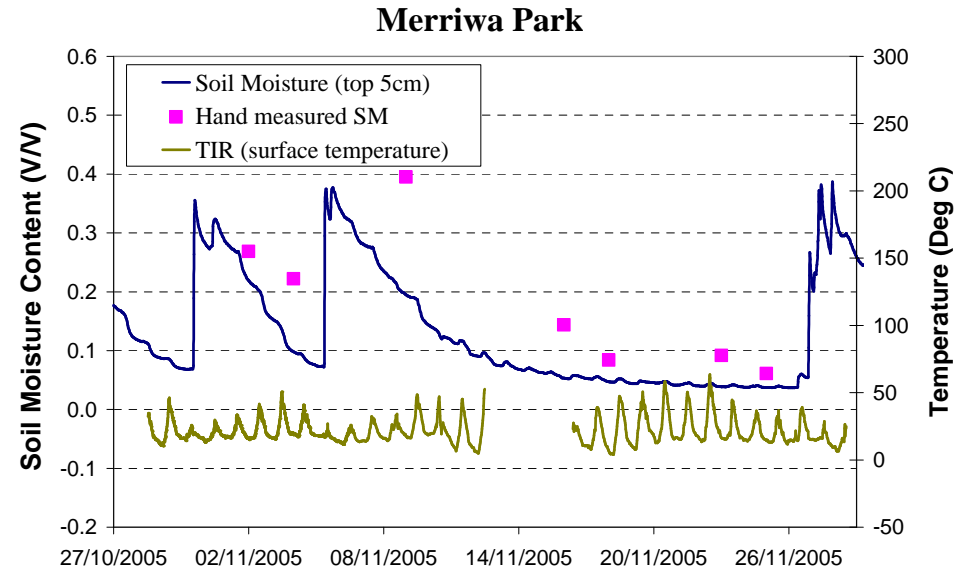


Figure 6d: Illustration of availability of all data at Merriwa Park

3.2.1 Soil Moisture Measurement

As illustrated in *Figure 6a-d*, soil moisture data consists of two sources; one is from the continuous measurements from each monitoring station, whereas the other source comes from the individual manual measurements on an irregular time basis. The measurements taken at the SM monitoring station were about 1km away from the TIR ground station (where the TIR data were taken) and are used for testing the presumed SM_{TG} relation. The hand measurements made near the TIR station site within 300m (hand measurements are available at *Illogan, Midlothian and Merriwa Park*). Because there is only a limited amount of hand measured soil moisture for this study, these hand measurements made at these sites are not directly used to test the $SM-T_G$ relation, but used as a means for verifying the representativeness of ground station measurements. As hand measurements were made very close to the TIR station, they are supposed to be approximately equivalent to the actual soil moisture of the thermal infrared site. So by comparing the ground station based SM data and hand measured SM data, the representativeness of the ground station based SM data to the TIR site can be determined.

Soil moisture data measured from ground station are the averaged value for the top 5 centimetres of soil layer. In this study, measurements performed at a single point at the station are used and corresponding to the areal weighted TIR measurement. Instead of every 5 minutes for thermal data, soil moisture is measured at 20-minute interval using the hydraprobe from 11/10/2005 to 31/12/2005. An average of the 3 measurements within an hour is taken for the hourly average soil moisture content.

Once properly calibrated, the hydraprobe allows accurate measurements of the soil water content. Although several soil moisture sensors have been installed in the site, this study will only consider the top 5 centimetres soil moisture content measured by the Hydraprobe. *Figure 7* below shows a schematic map of the installation of the soil moisture instruments in a typical site.

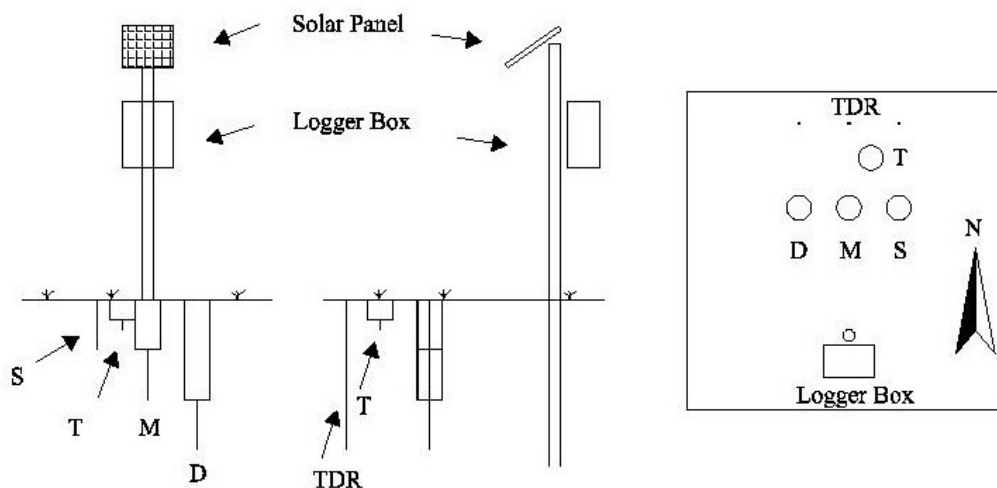


Figure 7. Schematic map of SM instrumental installation of study site. Although soil moisture were made at various depths, only the top 5cm SM data is concerned in this study.(Source: NAFE website)

After data calibration, it is noted that the soil moisture data contains some irregularly high SM values during rain days. Both lab and field experiments show that even in very wet conditions the hydraprobe should never give values higher than 0.5 V/V. Therefore, measured soil moisture contents which were greater than 50% v/v will be eliminated to prevent inconsistency.

3.2.2 Soil Moisture Infilling

A certain amount of soil moisture data has been missing for *Illogan*. However, an obvious downgrading trend between two successive rain events and a daily cycle pattern for soil moisture is observed from the data plot. As such, the missed data in any short periods where there is no rainfall was infilled using linear interpolation. *Figure 8* below shows the results of soil moisture infilling at *Illogan*,

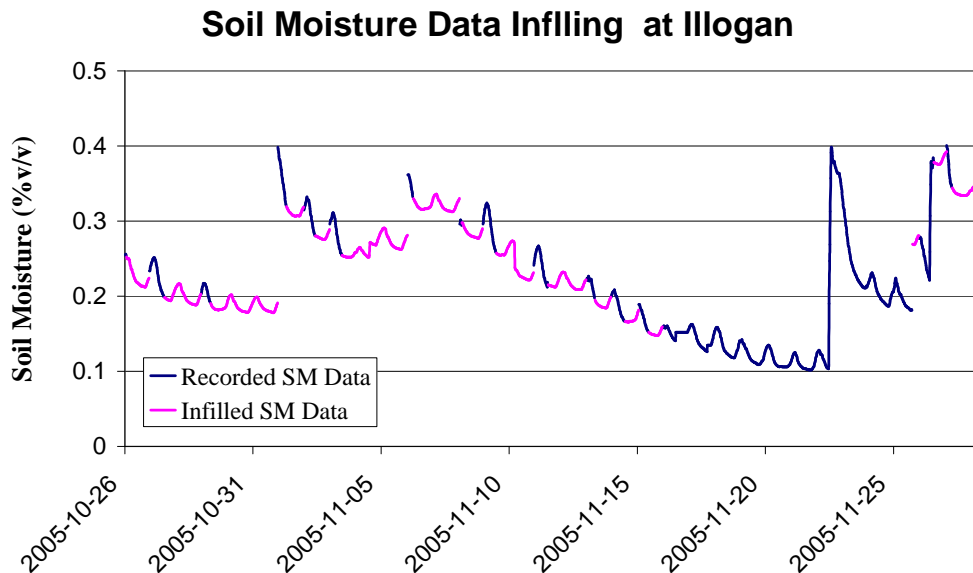


Figure 8: Soil moisture infilling for Illogan. A sudden increase in SM on the graph suggests there was a rainfall event.

3.2.3 Representativeness of Ground Station Based Soil Moisture

It is known that for *Illogan*, *Midlothian* and *Merriwa Park*, the soil moisture measurements were done at the stations which were about 1km away from their corresponding TIR stations. Therefore, individual hand measured soil moisture data taken at a closer distance (300m) from TIR stations are utilised in this study to test how representative the ground station based SM is to the TIR sites. *Figure 6a, c, d* shows the comparisons of the two types of soil moisture data.

It can be seen in *Figure 6b*, the hand taken SM measurements at *Midlothian* illustrates the best match to the ground station based SM measurements, which suggests a high compatibility of the SM data and TIR data at this site. *Illogan* (*Figure 6a*) shows a relatively high degree of similarity of soil moisture of 1km and 300m from the TIR site except for one measurement made on 02/11/05. However, it should be recognized that only four hand measurements were available for *Illogan*, so information is deemed not sufficient to make absolute judgment on the representativeness of the SM in this case. Station based SM data at *Merriwa Park* (*Figure 6d*) is least representative to the TIR sites as it exhibits a poor correlation with the hand measurement.

It should be noted that the information and discussions provided in this section are meant to aid the explanation for the analysis results in later sections and will not form a part of the methodology for the research.

3.2.4 Thermal Infrared Measurement

The four ground monitoring stations were supplying all the remote sensing data for this study in order to attain a higher degree of accuracy (avoid atmospheric correction procedures during remote sensing). *Figure 9* below shows a schematic map of the installation of the soil instruments in a typical site. The method for near surface soil moisture retrieval using thermal infrared sensors relies upon using the thermal infrared data to measure the soil surface temperature, as soil moisture influences the thermal properties of the soil (Walker, 1999). The thermal infrared sensors in the study sites firstly acquire the brightness temperature of soil surface; a conversion method is then applied to the brightness temperature to obtain the actual surface temperature using an emissivity factor.

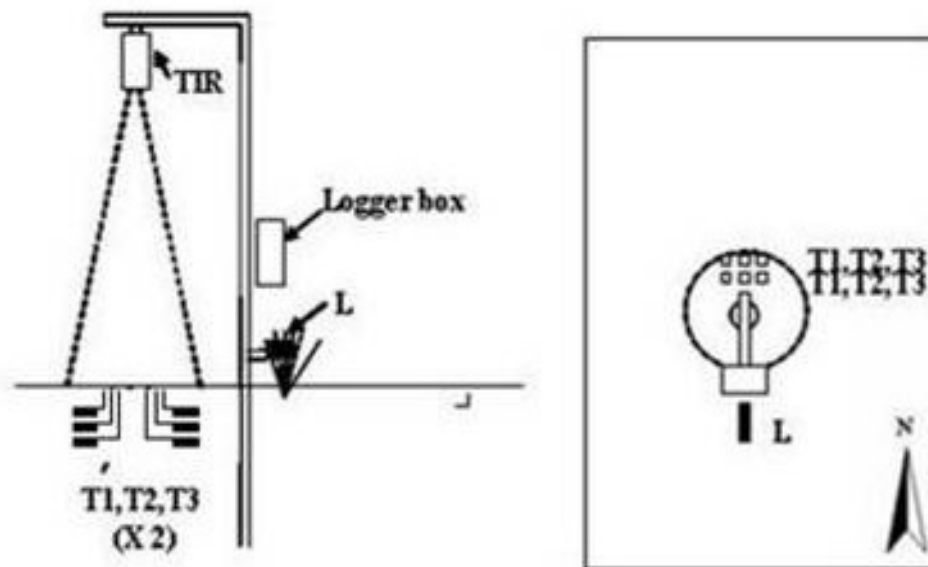


Figure 9. Schematic map of TIR instrumental installation of study site, showing soil temperature sensors at 1cm(T1), 2.5cm(T2) and 4cm (T3) depths, leaf wetness sensor (L) and thermal infrared sensor (TIR). (Source: NAFE website)

The radiometric temperatures from TIR data are the areal averaged value of the measured site. Thermal data was taken every 5 minutes from 26/10/2005-26/11/2005 (refer to *Figure 6a-d*) using the thermal band of 8-14 μ m wavelength. It has been calibrated in cold cycle and warm cycle against water target before and after campaign.

In the rare data set provided, the emissivity for surface temperature conversion is assumed equal to 1.0. Despite emissivity is essential for thermal infrared computation; it will ultimately be canceled out during the computation process in this study. Owing to this fact, any modification of emissivity will not influence the final results of the study, so value will not be further elaborated, and is assumed to be the original value 1.

No atmospheric corrections are applied to the thermal infrared data in this study. Unlike satellite operating in high elevation or orbits above the ground, ground monitoring station is installed on the near-ground level (usually a few meters above) so it is less likely to be affected by atmospheric disturbance such as cloud, grass fire (smoke) on the sensing process (i.e. it will not measure the surface temperature of the cloud top and fire).

As can be seen in *Figure 6a-d*, each site has certain gaps in the continuous thermal infrared measurement, which indicates some data were missing or not being measured for some reasons.

Illogan, Midlothian and Merriwa Park has minor amount of data missing, whereas *Stanley* has significant absent data for about 15 days, which accounted for half of the total length of the period being investigated. So the availability of the data to be used in the study does not guarantee the full length of the month. And this could be a major limitation of the research.

3.2.5 Surface Temperature Gradient T_G

Hourly surface Gradient is computed using the 13 T_s temperatures (i.e. 5 minutes interval) taken within an hourly period. Linear regression using least square fitting is utilised to calculate the gradient. The figure below illustrates the fundamentals of this calculation. *Figure 10* is an extraction from T_s data set for 0800-0900 period of 03/11/2005. It is noted from the graph that $T_G = 0.167$, with coefficient of determination (r^2) equal to 0.9798, which implies a constantly stable increase of surface temperature.

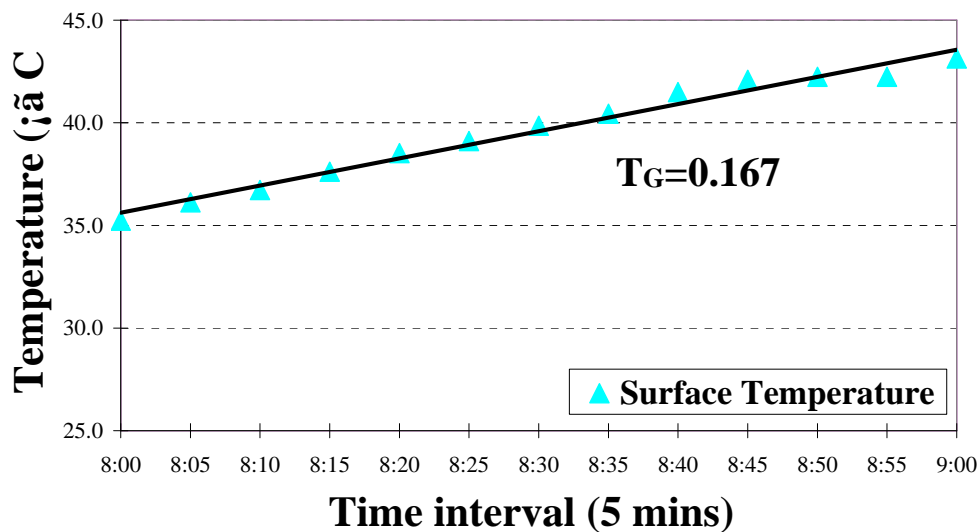


Figure 10: Illustration of T_s gradient computation using the temperature measurements within an hourly period. Gradient unit: Deg(C)/minute.

Due care was taken in filtering out the inconsistent temperature gradients that would have been affected by the cloud covers. Despite *Figure 10* above shows a nearly ‘perfect’ pattern of the change in temperature, this is not always the case in reality. Cloud has no impact on the instrumental measurement itself (i.e. an instantaneous measurement of surface temperature), but it will influence the hourly surface gradient T_G computation process. For example, the early morning (i.e. 0800-0900) temperature gradient is supposed to be positive in a cloud-free day due to the fact that the solar radiation is constantly increasing. But with the presence or partial/scattered presence of cloud, the gradient will vary irregularly as shown in *Figure 11* next page.

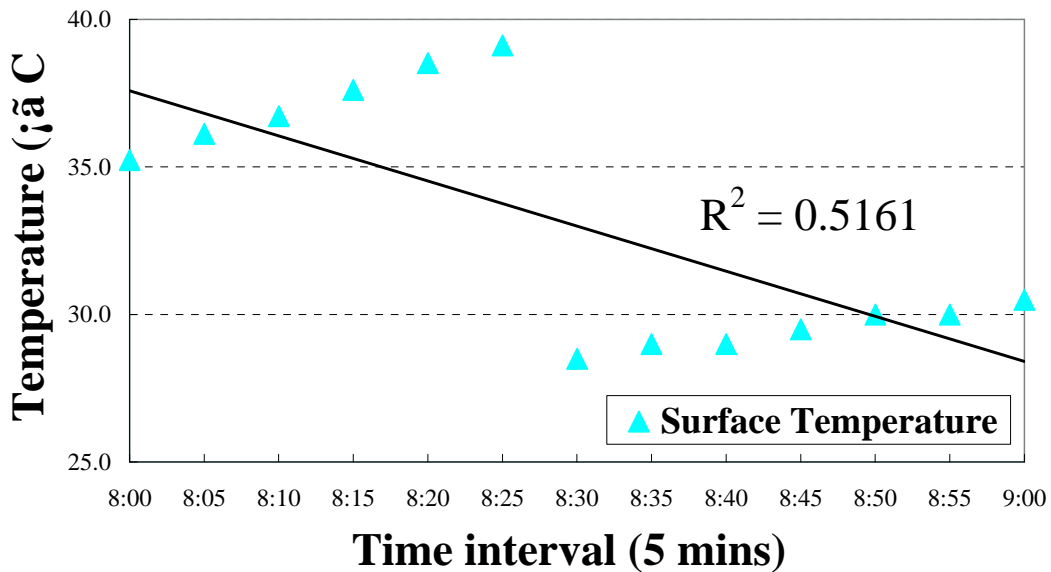


Figure 11. Graph illustrating T_G change (to negative) for the hourly period where the cloud is present after 0830. The fitted trend-line has an r^2 of 0.5161.

Figure 11 shows a circumstance where the negative T_G occurs due to the partial presence of cloud in the second half of the hourly period (i.e. from 0830-9000). The converse can also hold true for the afternoon period, in which the slope may happen to be positive due to the presence of cloud at given time intervals where the slope is supposed to be negative due to the decreasing solar radiation.

Another example can also be found where the overcast lasts for long period of time during the day. Thus the surface temperature variation during the day would be become smaller, which in turn reduces the temperature gradient. A cloud-free day and a overcast day is selected to illustrate this cloud impact in Figure 12 on next page, from which a flatter gradient is observed due to the presence of the overhanging cloud that block the incoming shortwave radiation from the sun.

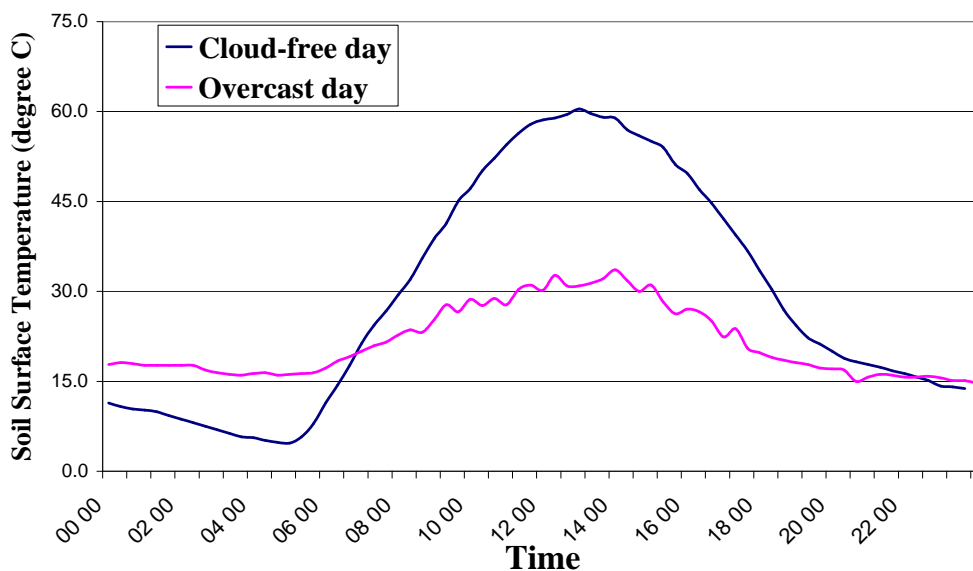


Figure 12. Graph illustrates the soil surface temperature change become smaller due to the presence of cloud during the day.

As Pegram's method implies that the temperature gradient change is solely due to the soil moisture content, it is essential to avoid using the gradients biased by the cloud to ensure the consistency of the data. The presence of cloud over any time during the day can be easily indicated by incoming

shortwave radiation. If the incoming shortwave energy (measured from the gauging station) remains at a relatively consistent trend and magnitude over a time period, it implies no cloud is present. On the contrary, if the measured shortwave radiation fluctuates during a time period, which means scattered cloud is present. A fully overcast day (i.e. cloud present for the whole day) is shown by a pattern of consistent trend but a lower magnitude. *Figure 13* illustrates these three different cloud cover situations.

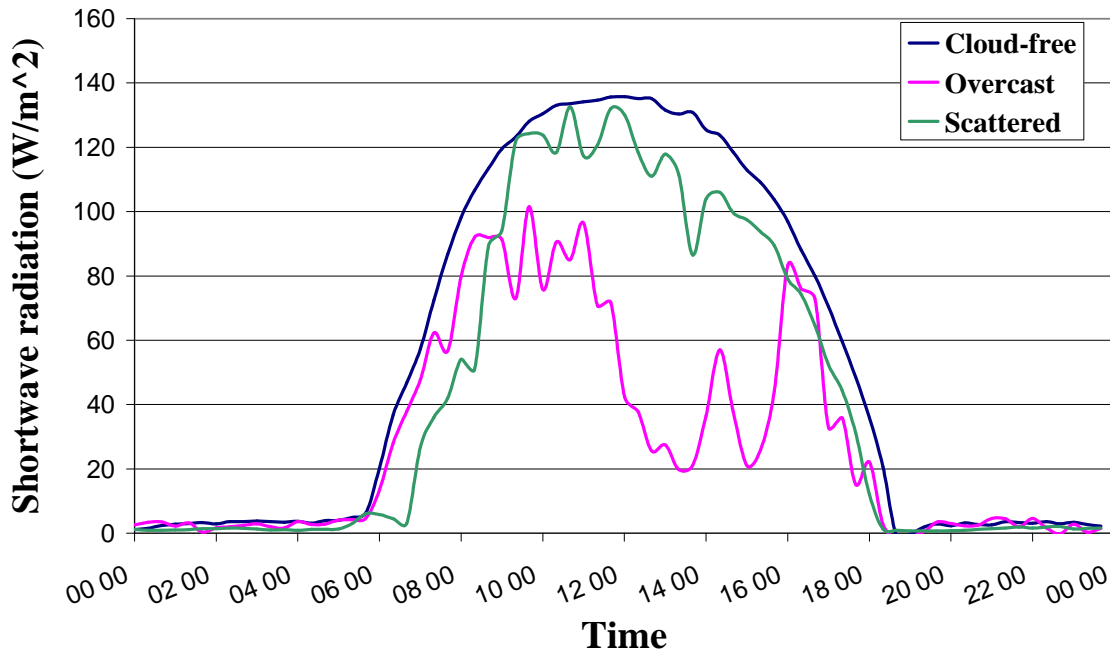


Figure 13. Illustration of the cloud-free, overcast and scattered cloud days according to different cloud cover conditions. Data is extracted from the shortwave solar radiation collected from Stanley site.

A manual classification system of the cloud condition is then carried out for each hourly period from 0700 to 2000 for each day using the shortwave radiation data set. Three classes are proposed for the system according to the cloud condition and its associated influences on the temperature gradient computation:

Class 1 – Cloud-free

This class includes the hourly periods that are cloud free, which have smooth shortwave radiation curve, such as the all the hourly periods on the “Cloud-free” curve in *Figure 13*. It is also noted that the 0700-0800 hourly period of the “Overcast” curve is also classified as cloud-free period owing to the fact it is not yet affect by the cloud cover. Similarly, 1500-1600, 1600-1700 and 1700-1800 on the “Scattered” curve are considered as cloud-free periods, as in this study it is assumed that the preceding scattered cloud will not have significant impacts on the temperature gradients.

Class 2 – Scattered (with no preceding overcast)

It contains the hourly periods which have partial presence of clouds, obvious fluctuations of shortwave radiation can be observed for the period. In *Figure 13*, 0900-1400 of the “Scattered” curve is classified into this class.

Class 3– Overcast

0900-1600 of the “Overcast” curve shows an apparent overcast situation as the detected incoming shortwave is consistently lower than the regular level. Except for the fully “overcast”, any hourly period after the overcast (even if it is cloud-free or has scattered cloud), it also falls into this class because the preceding overcast will influence greatly on the gradients for the

following hourly periods. Therefore, 1700-2000 of the “Overcast” curve is classified class 3.

The incoming shortwave radiation data is only available at *Stanley*, considering the close distance for the four study sites and the shortwave radiation is supposed to have little variation across the small area, it is assumed that the shortwave radiation data is applicable to all other three study sites.

After the classification, results are listed in *Figure 14*, *Figure 15* and *Figure 16* below, which illustrate the number of days identified for hourly periods from 0700-2000 under each class. It can be seen that the hourly periods (also the gradients) in morning and afternoon are less vulnerable to cloud influence. Scattered clouds are more likely to be present over the time periods at around midday, whereas morning and afternoon periods are mostly free of scattered cloud. In *Figure 16*, it is shown that the morning periods are less overcasted periods than that around the midday and after.

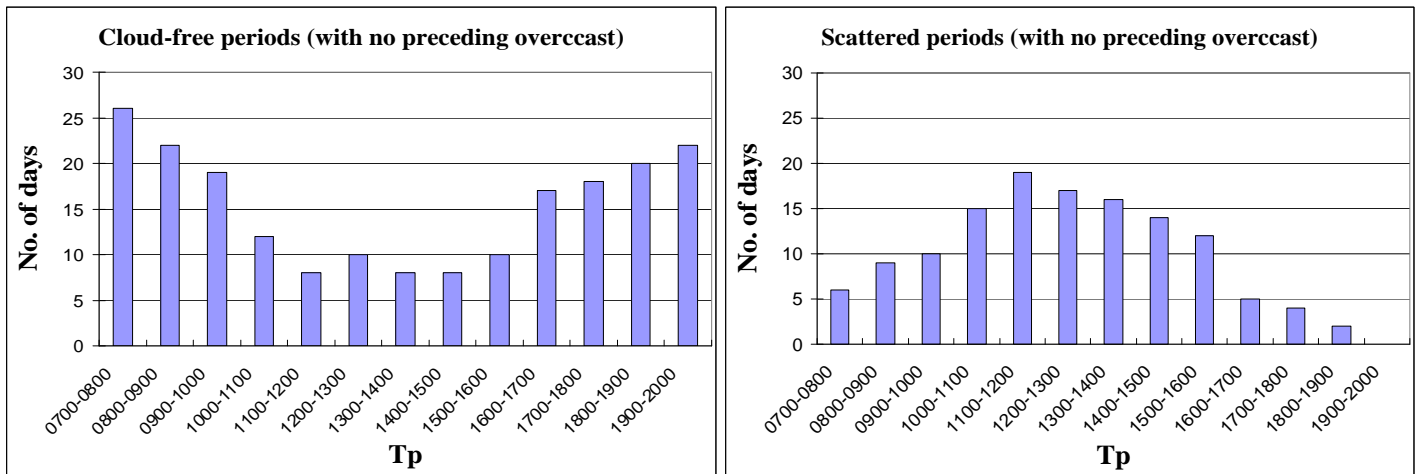


Figure 14. The number of days that each hourly period is experiencing cloud-free (Class 1) condition.

Figure 15. The number of days that each hourly period is experiencing scattered cloud (Class 2) condition.

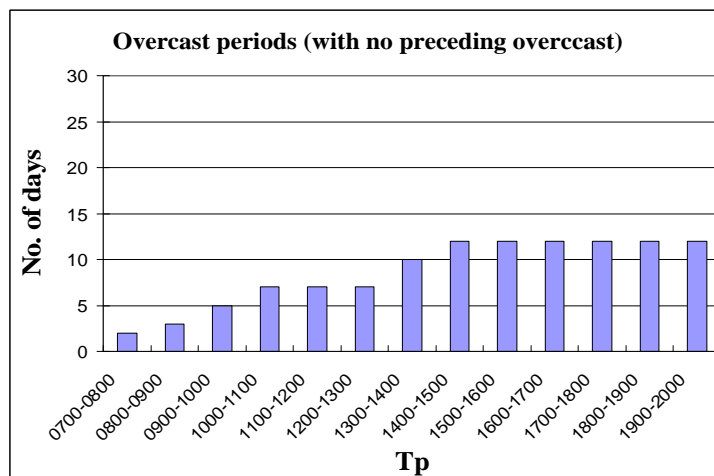


Figure 16. The number of days that each hourly period is experiencing overcast (Class 3) condition.

Since it is proved that the surface temperature gradients are more likely to be influenced by the scattered and overcast clouds. As a result, in order to achieve higher data reliability, and together with the fact that class 1 has the majority of the number of days (sufficient data for morning and afternoon periods), it is decided that only the Class 1 data (i.e. cloud free) will be retained for further use in testing the relationship.

4. Approach and Analysis

This section outlines the detailed methodology and analyses in approaching this research. The methodology is intended to form the basis for this research and describes the approaches to evaluation and verification (both graphically and statistically) of the Soil Moisture - Temperature Gradient relation in the study.

The primary aim of the study is to assess the impacts of different time period and land cover on the presumed linear model. For the evaluation purpose, each hourly interval with a specific land cover type will form a basic scenario for evaluation. For example, the surface temperature gradient and soil moisture relation obtained for 0800-0900 period over the native grass vegetation cover is considered as a scenario, the outcome of which is then compared with other scenarios to determine the best hourly period for each of the sites.

Some hourly periods during the day which are deemed inappropriate for the evaluation are firstly excluded according to the gradient conversion consistency. Three hourly periods around mid-day were eliminated. Together with the four different land cover, the remaining nine hourly periods form 36 scenarios to be evaluated. The evaluation of the scenarios consists of two parts: 1. a preliminary investigation into the SM-T_G relation using graphical representation. If any obvious linear relationships exist for certain scenarios, they can be observed from the graphical analysis. Range of T_G for each scenario is also being evaluated in this stage. 2. Systematical evaluation using statistical means. Coefficient of determination (r^2) and Root Mean Squared Error (RMSE) for each scenario are computed for evaluation. Best scenarios are nominated based on the results of the entire evaluation processes. *Figure 17: A schematic float chart outlines the procedures and methods for the study. Figure 17 below shows a schematic procedure which will be carried out for the study.*

A Schematic flow chart for Methodology

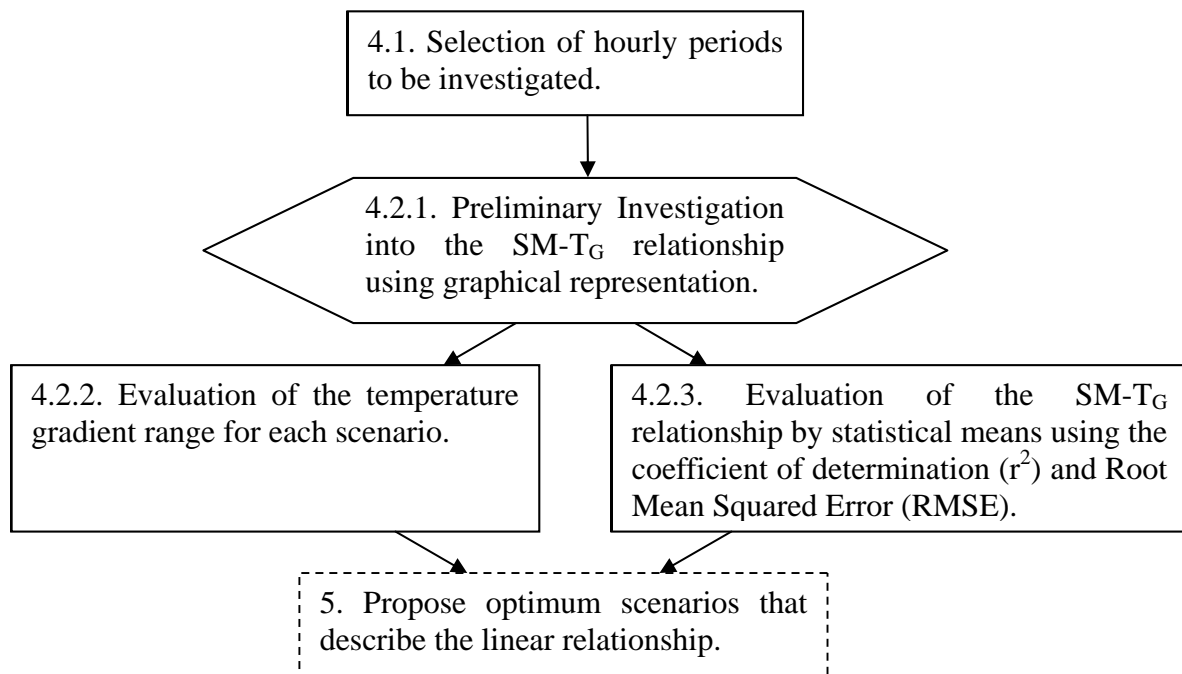


Figure 17: A schematic float chart outlines the procedures and methods for the study.

4.1 Selection of Desirable Hourly Periods

In this research, the hourly period will not only be confined in 0800-0900 as suggested by Pegram, but will be further elaborated to other suitable hourly periods during the day, in the hopes that an alternative hourly period which best describe the linearity could be found.

Provided the known field capacity and wilting point, the moisture content estimation using this relationship is mainly depending on the surface temperature gradients. So the correctness of the temperature gradients computation from the 13 measurements (5-minute interval for TIR data) has to be insured. As such, for hourly periods that are less likely to provide precise gradient computation will be firstly eliminated.

During the night time, thermal signature of ground soil is greatly reduced relative to day time due to the absence of sunlight. This reduction will lead to the outcome that the measured hourly TIR temperature range becomes narrower (hence the T_G), which could possibly worsen the accuracy of the computed result using the presumed Temperature Gradient-Soil moisture relationship. So it is preferable that the hourly temperature range is large enough to overcome its subtle sensitivity on the soil moisture prediction (which might leads to large errors). As such, night time between dusk and dawn (i.e. from 1800-0700) will be firstly excluded from being investigated.

In addition to the exclusion of nighttime, previous knowledge has proved that during the day, time periods at around mid-day are more likely to have fluctuated temperature gradients. This is because in the morning, temperature is supposed to remain an inclined trend (temperature rising) until midday. The opposite also holds true for the afternoon when the temperature keeps falling down. Theoretically the morning temperature gradient should be positive and afternoon gradient be negative. The inconsistent bit always occurs when the gradients change from positive gradient to negative gradient around midday. *Figure 18* on next page illustrates that around mid-day, both negative and positive gradients appear for particular hourly periods, whereas in the morning and afternoon, gradients are consistently being within the positive and negative range, respectively.

As such, hourly periods during the night and around midday are excluded. The selected hourly periods to be used in the evaluation phases are listed as follows:

- Morning warming period from 0700 to 1100 (4 hourly periods)
- Afternoon cooling period: 1500-1900 (5 hourly periods)

The nine hourly periods have shown a higher degree of data consistency and hourly TIR temperature range, which will then be used in the presumed relationship, with the four different land cover types to form 36 possible scenarios.

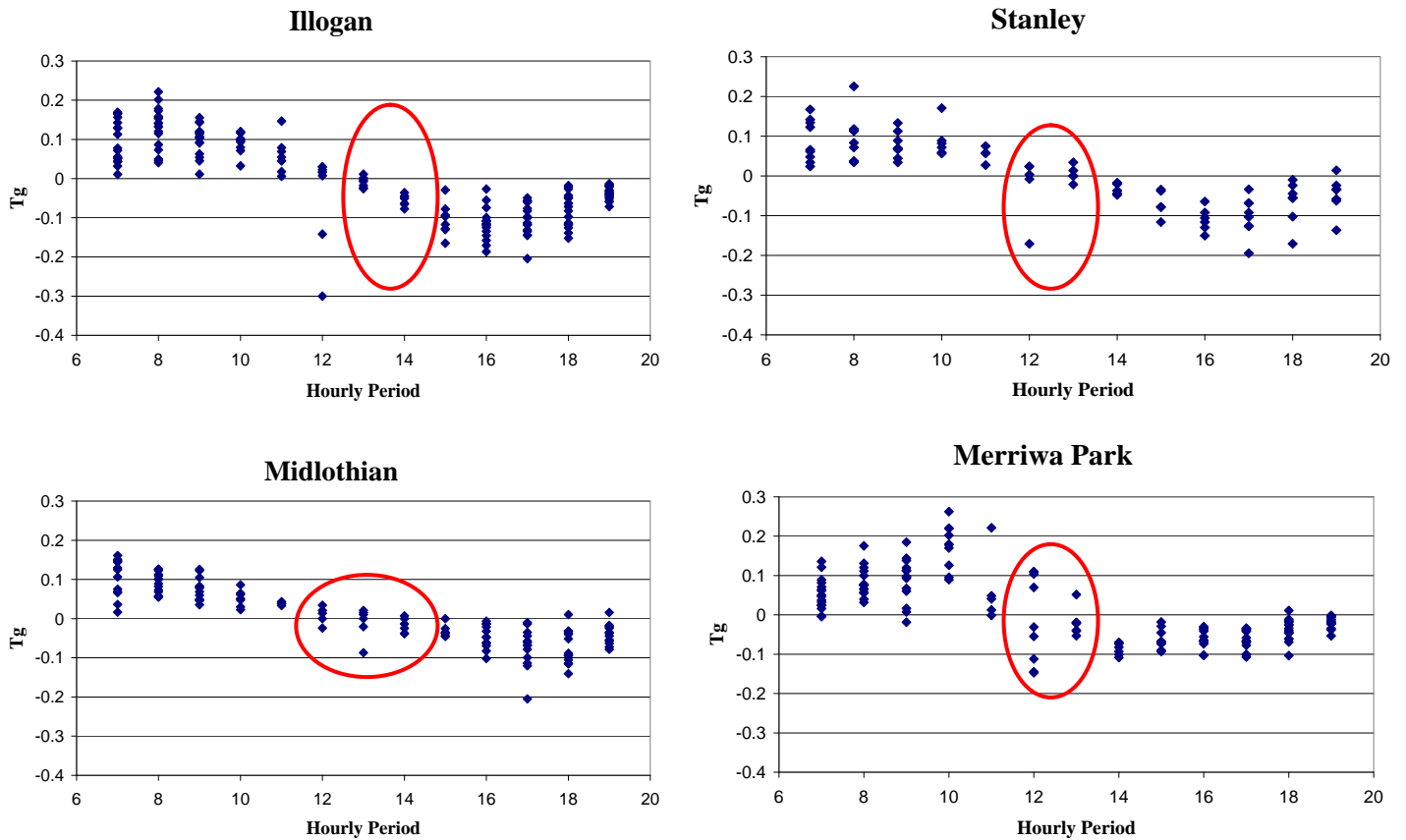


Figure 18. Plots of temperature gradient against each hourly period during the day. The red ellipses show the excluded periods around midday which have inconsistent gradients.

4.2 Methods for Scenario Evaluation

In total, 36 scenarios are generated and available for evaluation. Two evaluation methods are proposed: preliminary graphical analysis and statistical analysis. The graphical means provides a general insight of the SM and T_g relationship and an initial judgment on the whether the relationship of each scenario can be established in a linear manner. Statistical analysis involves the utilisation of the coefficient of determine (r^2) and the root mean square error (RMSE) to determine the linearity of the relationship.

4.2.1 Preliminary Screening

Analysis of the presumed model needs to consider the correlation of soil moisture contents and temperature gradients for each hourly period. In order to provide an initial screening of the scenarios, soil moisture contents are categorized into a series of soil moisture band of 5% interval and arranged against temperature gradients in *Figure 19a-d*. Hourly periods are indicated by the starting time (e.g. 7 represents the 0700-0800 hourly period) on the graphs. It should be noted that the temperature gradient of afternoon periods is presented as positive (i.e. absolute value) in *Figure 19a-d* despite the actual gradients were negative. This is because the gradient in the presumed model only denotes the extent of temperature changes; the soil moisture is said to depend on the magnitude of the gradient but not the convention. By arranging the negative gradients to positive, it eases the comparisons between morning periods and afternoon periods.

Illogan

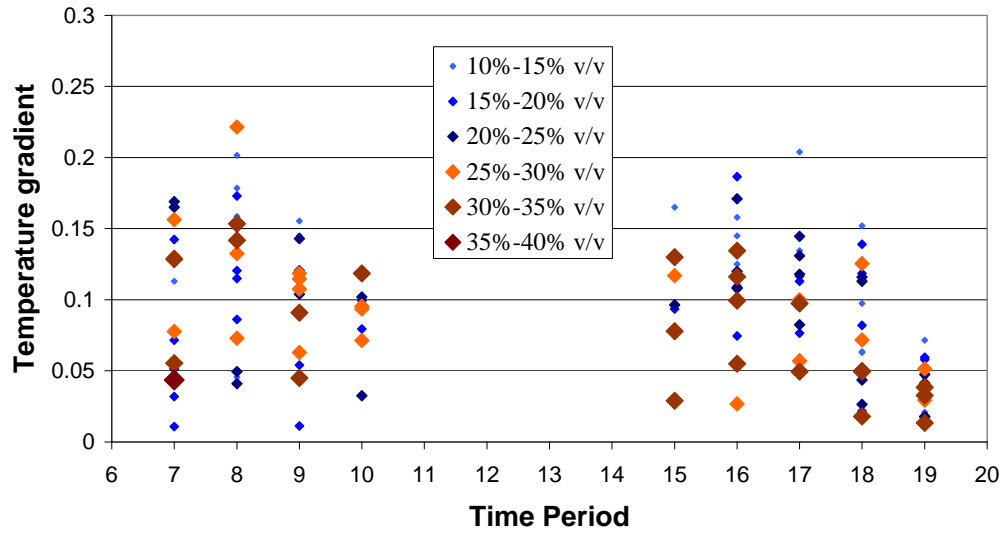


Figure 19a: Graphical representation of the SM-TG relation for Illogan.

Stanley

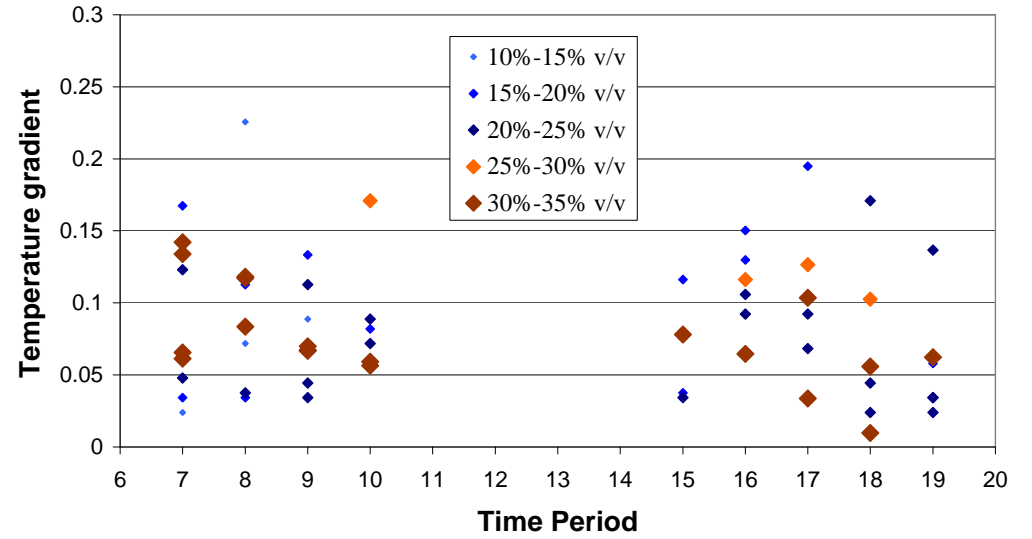


Figure 19b: Graphical representation of the SM-TG relation for Stanley

Midlothian

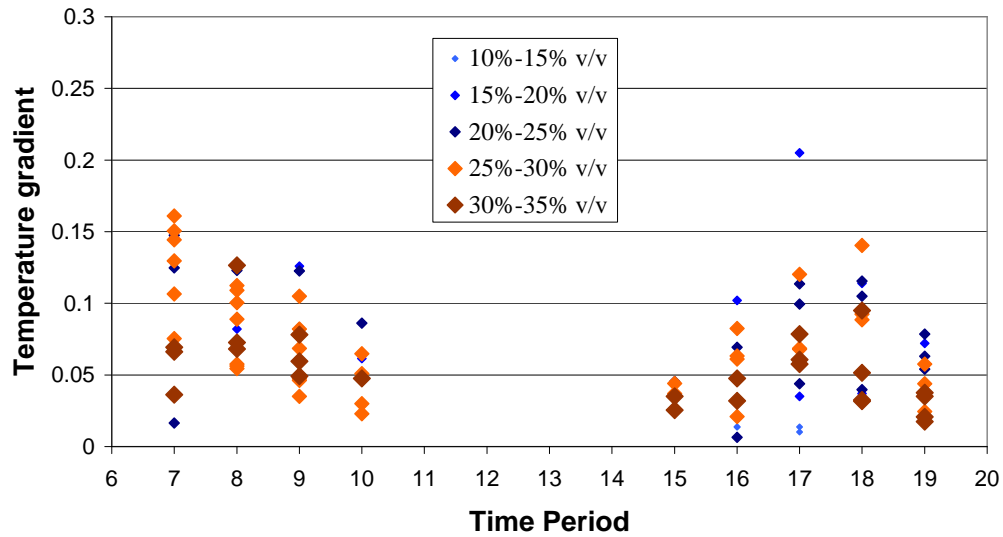


Figure 19c: Graphical representation of the SM-TG relation for Midlothian.

Merriwa Park

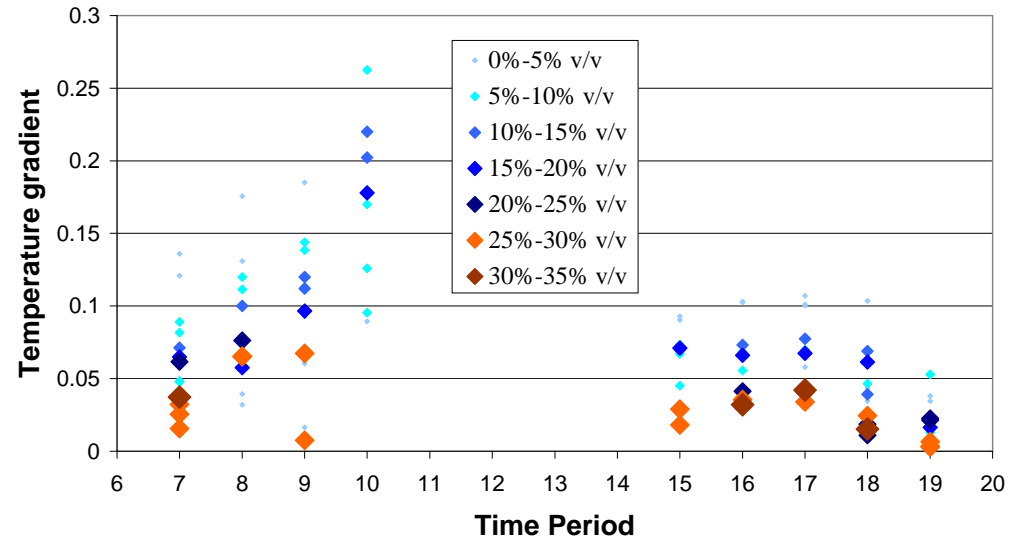


Figure 19d: Graphical representation of the SM-TG relation for Merriwa Park.

According to Pegram (2006)'s methodology, it stated that the temperature gradient on a particular area for a fixed period of time would be inversely related to the average soil moisture content over the area. That is, a greater temperature gradient should correspond to drier soil whereas a smaller gradient correspond to a wetter soil. If this relationship holds true, from the graphical representation in *Figure 19a-d*, the soil moisture bands of smaller soil moisture are supposed to be corresponding to larger temperature gradients (i.e. in higher position along y-axis for each hourly period), and with greater soil moisture bands in lower y-axis. No overlapping of different soil moisture bands should occur provided that the presumed relationship perfectly holds. Thus, an established relationship in the graph should have the following features:

- No overlapping of different SM bands
- Well ordered soil moisture bands for each hourly period, with lower soil moisture bands positioned higher along y-axis and higher soil moisture bands in lower y-axis.

Summary of results for each site from *Figure 19a-d* is provided in *Table 1*.

Table 1: Summary of graphical interpretations for each site

Site	Observable results from graphical analysis
Illogan	The soil moisture contents ranging from 10% v/v to 40% v/v were measured in <i>Illogan</i> site. However, no obvious trend of the soil moisture bands is observed for all hourly periods.
Stanley	No well ordered the SM bands was found in <i>Stanley</i> . Distribution of soil moisture bands does not indicate any correlations.
Midlothian	Majority of soil moisture content in <i>Midlothian</i> varied from 20% v/v to 35% v/v. Despite more apparent relationship between SM and T_G is seen for <i>Midlothian</i> than <i>Stanley</i> . Overlapping and scattering of SM bands occur for all hourly periods.
Merriwa Park	Scenarios at <i>Merriwa Park</i> deliver more convincing distributions of SM bands compared to other sites. However, no perfect trend is found for the soil moisture band. It is noted that more irregularities occur for the lower soil moisture bands, where the low soil moisture bands ranges from low gradients to very high gradients.

Results of the graphical interpretation have not yet verified the correctness of presumed relationship for any of the scenarios. One of the reasons could be the possible occurrences of some individual SM or TIR measurement errors, which worsen the distribution of the soil moisture bands against temperature gradients in graphical presentations. As such, even if a linear relation exists for soil moisture and temperature gradient to some extent, it cannot be clearly observed in the graph. Nevertheless, this could be remedied by using statistical means in analyzing the data and is carried out in *Section 4.2.3*.

Another likely reason could be that the presumed SM- T_G relationship actually does not hold for some scenario, so that it does not show any of consistent trends or distributions of SM bands. Again, this requires more supporting evidence from analyses by other means.

4.2.2 Temperature Gradient (T_G) Range

As mentioned in *Section 2.3.3*, the maximum and minimum T_G values define the T_G range and correspond to the observed driest soil and wettest soil respectively. A small range of T_G may give large errors in soil moisture estimation because a slight uncertainty in gradient value will lead to large soil moisture difference. Therefore, for a particular SM- T_G relationship, a wide temperature gradient range will be more desirable for accurate soil moisture estimations. *Figure 20a-d* on next page shows the T_G range and associated deviations for each scenario. The maximum and the minimum T_G for each scenario correspond to the average value of the lowest SM band and the highest SM band defined in *Figure 19a-d*. Initially, the T_G range should be defined by the difference between maximum and minimum T_G values within the data pool (these maximum and minimum values are meant to correspond to the minimum and maximum soil moisture contents respectively). However, it is noticed that in *Figure 19a-d*, the soil moisture contents within a SM band do not distribute in an organized manner, some low soil moisture bands unexpectedly correspond to small temperature gradients and high soil moisture bands correspond to large temperature gradient, which leads to a large deviation while defining the T_G range. Therefore, average values of the two extreme SM bands were taken into account for this variance of temperature gradient. The Errors bars associated with each curve indicate the T_G deviations within the lowest and highest SM bands.

As such, the optimum scenario that produce least estimation errors shown in *Figure 20a-d* should have the large range of T_G whilst the T_G deviations small. Summary of results for each site from *Figure 20a-d* is provided in *Table 2*.

Table 2: Summary of temperature gradient range for each site

Site	Observable results from T_G range analysis
Illogan	Although the gradient ranges are moderate, deviations of T_G is large for all hourly periods, which indicates a possible poor linearity.
Stanley	A good scenario (1600-1700) has been identified, which shows small deviations and large range of T_G .
Midlothian	T_G Deviations are relatively small for all hourly periods compared to <i>Illogan</i> . 0900-1000 shows wide and acceptable deviations.
Merriwa Park	Large deviations from lowest SM bands noticeable for all hourly periods except 1500-1600. 1500-1600 also shows a large range of T_G .

The following scenarios which have wide T_G ranges have been identified in *Table 3* below. It should be mentioned that the ‘wide’ T_G range is a relative term and do not have an absolute threshold for selection.

Table 3: Scenarios with wide temperature gradient ranges

Site	Hourly Period	T_G Range
Illogan	-	-
Stanley	1600-1700	0.0756
Midlothian	0900-1000	0.0637
Merriwa Park	1500-1600	0.0681

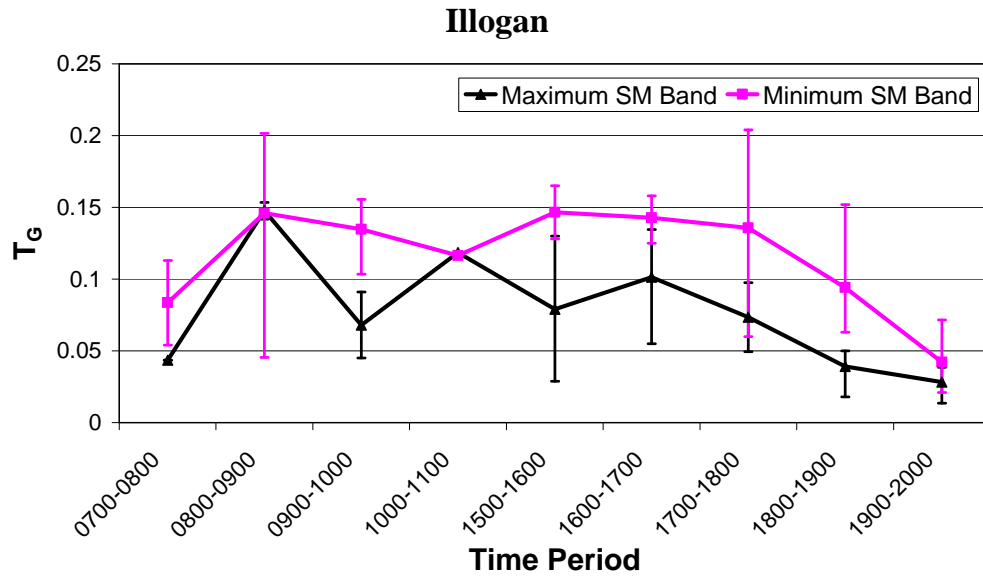


Figure 20a: Range of T_G and T_G deviations for each hourly period at Illogan

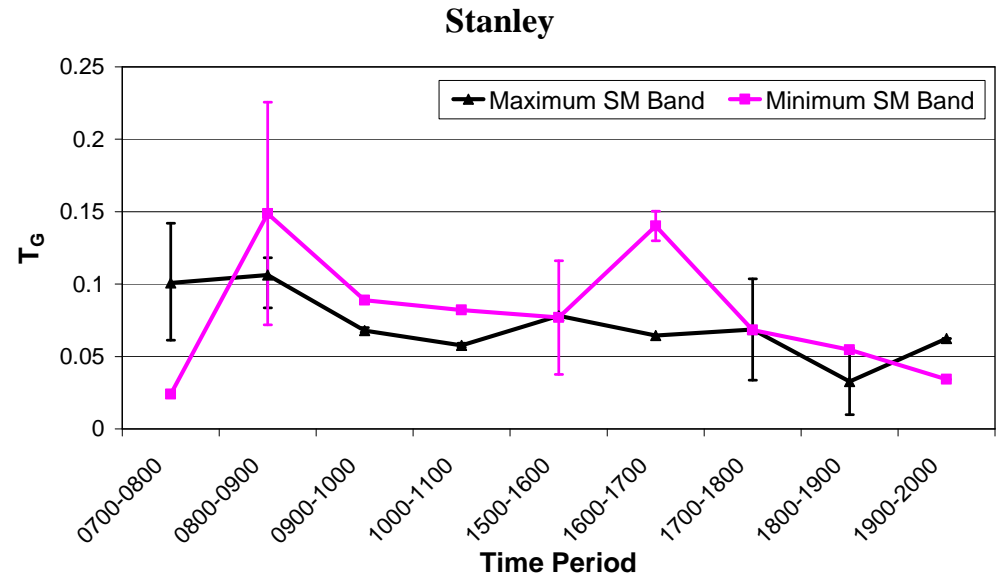


Figure 20b: Range of T_G and T_G deviations for each hourly period at Stanley

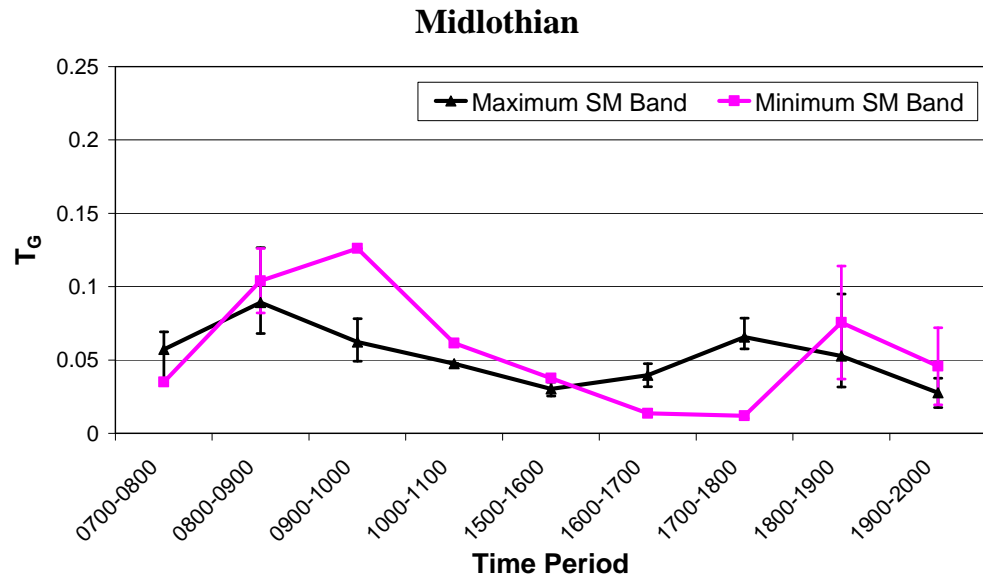


Figure 20c: Range of T_G and T_G deviations for each hourly period at Midlothian

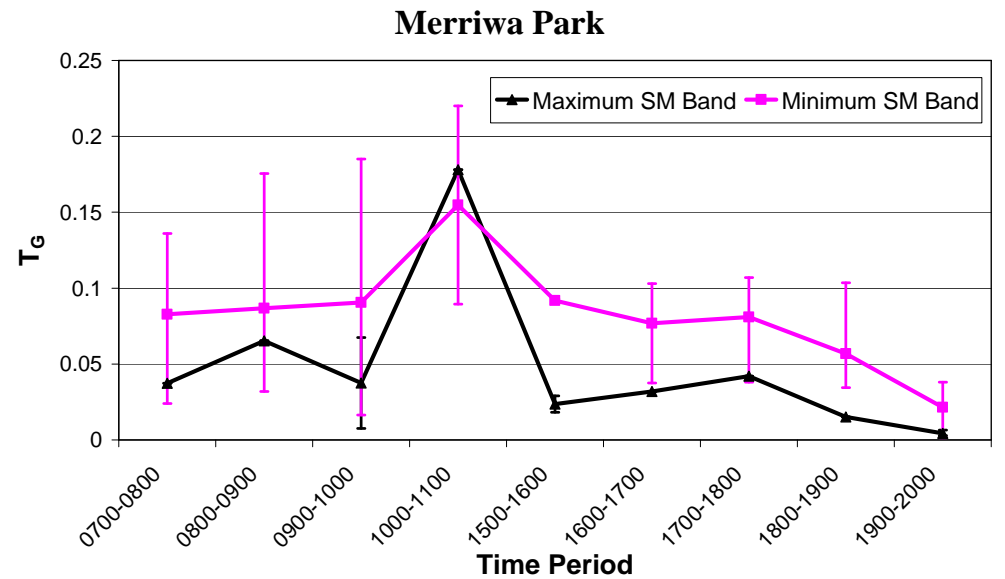


Figure 20d: Range of T_G and T_G deviations for each hourly period at Merriwa Park

4.2.3 Statistical Analysis

Coefficient of Determination (r^2)

In the context of this study, the coefficient of determination is designated to assess the proportion of the fluctuation of the soil moisture which is predictable from the temperature gradient. It is a measure that enables us to determine how certain soil moisture can be in making predictions from the presumed linear model. If the relationship can be confirmed, a r^2 value of close to 1 should be obtained. A value approaching zero indicates that the soil moisture and temperature gradient is poorly correlated.

r^2 is computed for each of the selected scenarios for all study sites. Results of the coefficient of determination are shown in *Table 4* and *Figure 21* below.

Table 4: Tabulation of r^2 for selected hourly periods for all study sites

Hourly Period	Illogan	Stanley	Midlothian	Merriwa Park
0700-0800	0.0165	0.1159	0.0080	0.2006
0800-0900	0.0010	0.0350	0.0876	0.0718
0900-1000	0.0704	0.1600	0.6014	0.1413
1000-1100	0.0604	0.0829	0.3923	0.1812
1500-1600	0.3128	0.0085	0.1287	0.6834
1600-1700	0.1816	0.8288	0.0450	0.2758
1700-1800	0.1499	0.1247	0.0438	0.2255
1800-1900	0.1306	0.0650	0.0245	0.3850
1900-2000	0.0829	0.0101	0.3126	0.2110

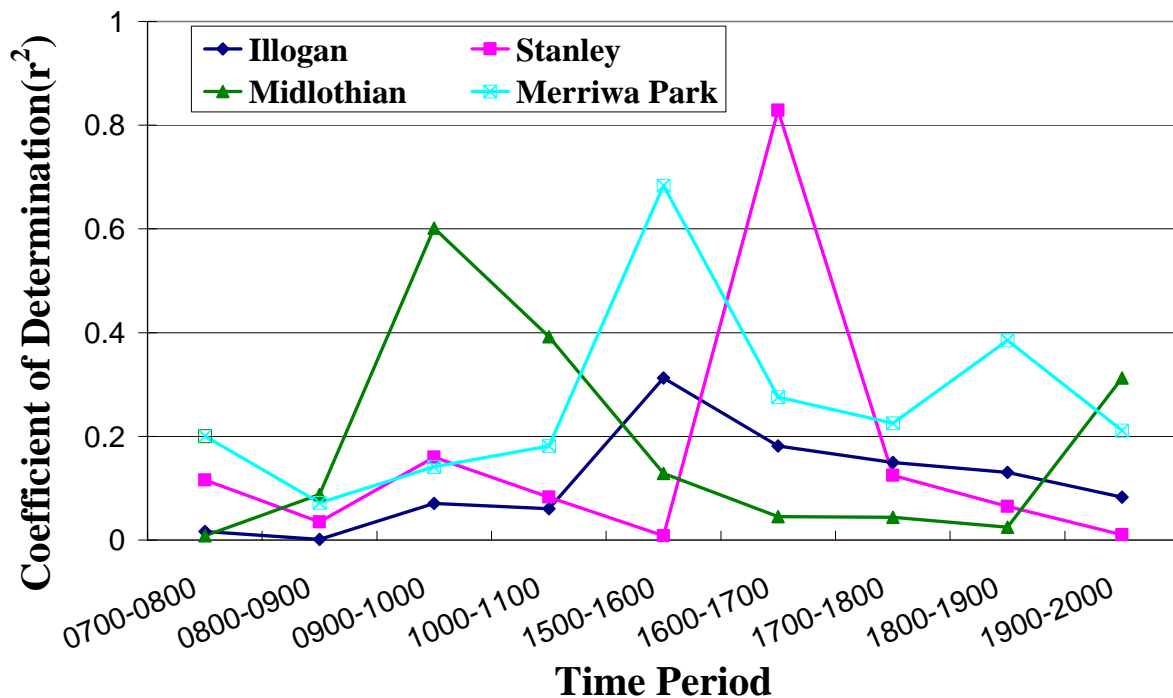


Figure 21: Graphical comparison of the relative magnitude of r^2 for all sites.

It can be seen from *Figure 21*, three scenarios show good correlations ($r^2 > 0.5$) between the soil moisture and temperature gradients: *Merriwa Park* (1500-1600), *Midlothian* (0900-1000) and *Stanley* (1600-1700), whereas all other periods were poorly correlated. All hourly periods for

Illogan do not show a convincing correlation. But it is noted that the 0900-1000 and 1000-1100 periods (consecutive) at *Midlothian* shows relatively good correlation, which indicate a consistent relationship between SM and T_G may occur during the 0900-1100 period. *Table 5* provides a summary of the scenarios with the highest r^2 value.

Table 5: Scenarios with highest coefficient of determination r^2

Site	Hourly Period	r^2
Illogan	-	-
Stanley	1600-1700	0.8288
Midlothian	0900-1000	0.6014
Merriwa Park	1500-1600	0.6834

Although three scenarios have been observed by evaluating the r^2 value, it raises another bias that associates with the use of r^2 , that is, r^2 always increases when a new term is added to a model, unless the new term is perfectly co-linear with the original terms. Adding a new term to the model will never decrease r^2 . This suggests that a scenario which has more data points (it is mentioned in earlier sections that due to missing thermal infrared data, different scenario might have different amount of available data to be used) is possibly placed in an inferior position in showing a high r^2 value. As such, the Root Mean Squared Error (RMSE) which is able to attenuate this impact will be used to verify the presumed model.

Root Mean Squared Error (RMSE)

As the name suggests, Root Mean Squared Error is just the square root of the mean square error. It is used here instead of Mean Squared Error since it has the same units as the quantity plotted on the vertical axis (i.e. %v/v) and statistically, it gives the magnitude of errors we will possibly get from the fitted linear regression between soil moisture and temperature gradient. The smaller the RMSE, the smaller SM estimation errors will be from the fitted linear relationship. As RMSE is taken from the mean errors, it provides an unbiased statistical interpretation of linearity of the relationship, or in another words, it is not affected by the number of data present in each scenario. Results of computed RMSE are shown in the *Table 6* and *Figure 22* below:

Table 6: Tabulation of RMSE values for selected hourly periods for all study sites

Hourly Period	Illogan	Stanley	Midlothian	Merriwa Park
0700-0800	0.068	0.067	0.052	0.088
0800-0900	0.065	0.079	0.040	0.078
0900-1000	0.065	0.067	0.024	0.076
1000-1100	0.058	0.057	0.027	0.041
1500-1600	0.070	0.062	0.059	0.047
1600-1700	0.067	0.024	0.061	0.076
1700-1800	0.060	0.059	0.063	0.077
1800-1900	0.062	0.062	0.048	0.079
1900-2000	0.066	0.056	0.042	0.085

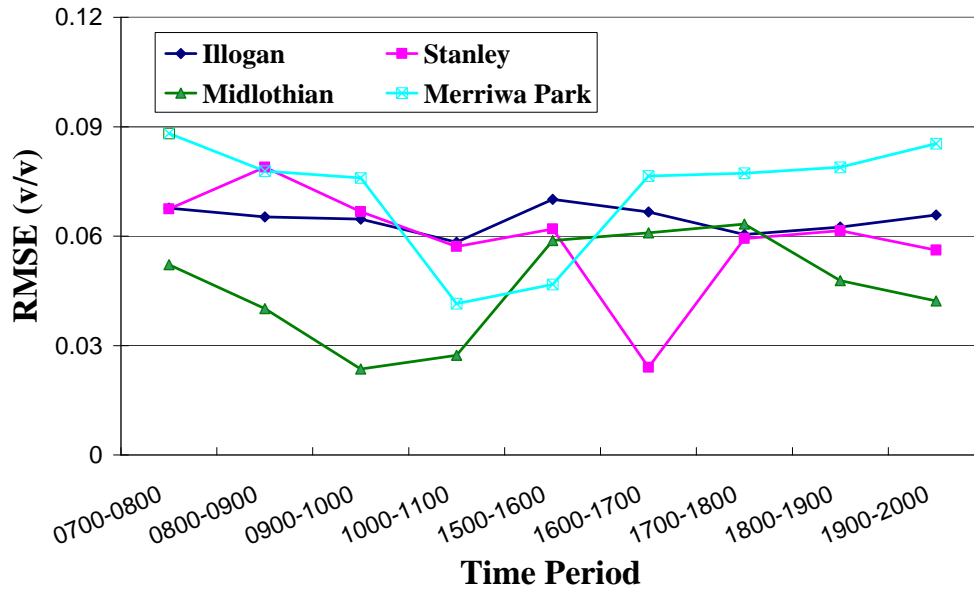


Figure 22: Graphical comparison of the relative magnitude of RMSE for all sites.

The results illustrate that the three scenarios have root mean squared errors less than 3% (selection of 3% is arbitrary; it only shows a relative scale): *Stanley*(1600-1700), *Midlothian*(0900-1000) ad *Midlothian* (1000-1100). Estimation of soil moisture from the linear relationship established by the SM and T_G data in these scenarios will have a mean 3% error from the actual measured value. Again, *Illogan* (bare soil) does not demonstrate good correlation for all hourly periods using RSME analysis, and the result agrees with the result of r^2 analysis. The two consecutive hourly periods from 0900-1100 at *Midlothian* exhibit low RMSEs for the presumed relations, correspondingly, they also possess higher degrees of linearity depending on r^2 values.

A discrepancy between r^2 and RMSE analysis is noticed for the scenario of 1500-1600 at *Merriwa Park*, where it exhibits high degree of linearity but relatively large RMSE (large estimation errors using the linear relationship). This is because although the high value of the coefficient of determination indicates a good fit of the sample mean to the regressed mean for scenario, it does not guarantee a good fit to the entire data set.

In summary, scenarios with low root mean squared errors (RMSE <3%) are summarized in the following table:

Table 7: Scenarios with lowest root mean squared error (RMSE)

Site	Hourly Period	RMSE(v/v)
Illogan	-	-
Stanley	1600-1700	2.4%
Midlothian	0900-1000	2.4%
	1000-1100	2.7%
Merriwa Park	-	-

5. Result and Discussion

Section 4.2 evaluated the suitability of linear relationship in all selected scenarios against 3 criteria: 1. wide range of surface temperature gradient within the relationship; 2. Linearity using coefficient of determination (r^2) and 3. Linearity and estimation error using Root Mean Squared Error (RMSE) of the relationship. A number of scenarios were proposed which have the best results against each of these criteria. The overall optimum scenario will be generated based on the combination of considerations of these three criteria. Effects of different hourly periods and vegetation cover on the presumed relation are also discussed in the following sections.

5.1 Optimum Scenario

Table 8 summarized the proposed scenarios in earlier sections, which are based on the criteria of wide T_G range, high r^2 and small RMSE.

Table 8: Summary of proposed scenarios based on the three criteria

Site	Hourly period	T_G Range	r^2	RMSE(v/v)
Illogan	-	-	-	-
Stanley	1600-1700	0.0756	0.8288	2.4%
Midlothian	0900-1000	0.0637	0.6014	2.4%
	1000-1100	-	-	2.7%
Merriwa Park	1500-1600	0.0681	0.6834	-

It can be seen from *Table 8*, candidates (scenarios) proposed by RMSE are slightly different from the T_G range and r^2 , where as T_G range and r^2 suggested the same scenarios. The similarity of the suggested scenarios for T_G range and r^2 comes from the fact the deviations of T_G from lowest and highest SM bands were also taken into account while computing the T_G range. The deviations some how reflect the linearity of the SM- T_G relationship because less T_G deviations for the SM bands, the more likely it has well arranged SM bands (*Section 4.2.1 - 4.2.2*). The reason for differences between RMSE and the other two criteria were introduced in *Section 4.2.3*.

Taking the consideration of these three criteria, it can be concluded the *Stanley* (1600-1700) and *Midlothian* (0900-1000) are the two optimum scenarios that can be used for soil moisture retrieval with the linear relationship whilst generating the least possible estimation errors. It should be mentioned that the selection of good r^2 (>0.5) and RMSE ($<3\%$ v/v) are completely arbitrary in the context of this study (although higher r^2 and lower RMSE values are more desirable), however, they can be modified if a more/less accurate estimation were required for different purpose. Therefore, optimum scenarios may also change in accordance to different values for r^2 and RMSE taken.

Stanley (1600-1700)

The SM- T_G relationship of Stanley (1600-1700) is shown in Figure 23 below:

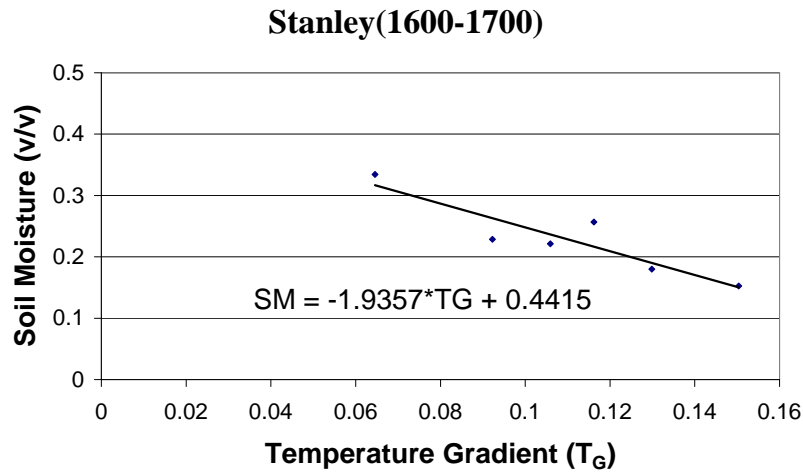


Figure 23: SM- T_G relationship for Stanley (1600-1700), the linear relationship is depicted by the equation $SM = -1.9357 * T_G + 0.4415$

Known temperature gradients are applied into the established linear relationship ($SM = -1.9357 * T_G + 0.4415$) to predict the soil moisture content. A comparison has been made to the predicted SM value and actual measured values are provided in Figure 24. The estimated soil moisture contents have a RMSE of 2.4% compared to the actual measured SM using the linear relationship.

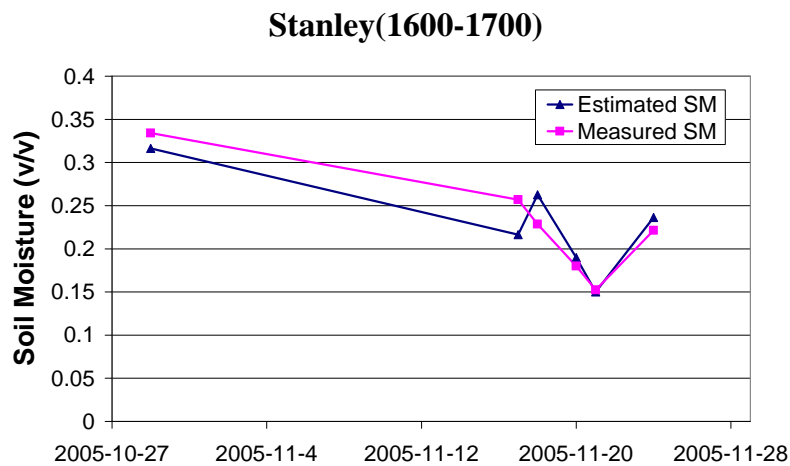


Figure 24: Comparison of estimated soil moisture and recorded soil moisture for Stanley (1600-1700). The gap between the first data point and second point illustrates the period of absent TIR data.

Despite Stanley (1600-1700) has a very good ability in estimating soil moisture with the linear relationship, it is noticeable that the relationship is based on the limited amount of data. This is because for Stanley site, a large amount of TIR data were missing (refer to Figure 9b) and some data which occur in cloudy days were excluded (refer to Section 3.2.4). Nevertheless, the scarcity of available data should not undermine the verification of the relationship for this scenario since Stanley had the TIR measurement and SM measurement being carried out at the same locations, which implied that the soil moisture measurements are most representative to the TIR site where temperature gradients were computed. In addition to the representativeness of soil moisture, the vegetation at Stanley is native grass, which has the second least dense canopy cover among the four

sites (*Illogan* is bare soil which has no vegetation). The low-density of the canopy cover also suggests a larger potential for thermal infrared to pass through vegetation and to accurately measure the surface temperature. Further, the shortwave radiation data which was used to classify the cloud condition (in *Section 3.2.4*) was also taken from the *Stanley* site, which gives the best indication on the cloud conditions at *Stanley* site.

Midlothian (0900-1000)

The SM- T_G relationship of *Midlothian* (0900-1000) is shown in *Figure 25*:

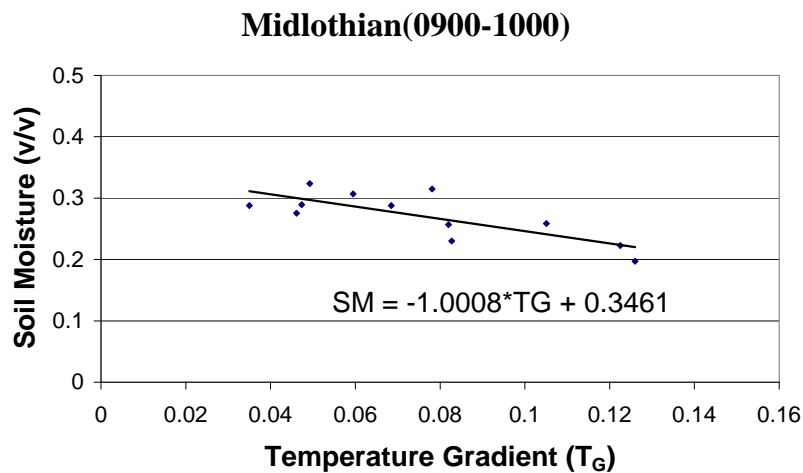


*Figure 25: SM- T_G relationship for Midlothian (0900-1000)), the linear relationship is depicted by the equation $SM=-1.0008*T_G+0.3461$*

Known temperature gradients are applied into the established linear relationship ($SM=-1.0008*T_G+0.3461$) to predict the soil moisture content. A comparison has been made to the predicted SM value and actual measured values are provided in *Figure 26*. The estimated soil moisture contents have a RMSE of 2.4% (same as *Stanley*(1600-1700) scenario) compared to the actual measured SM using the linear relationship.

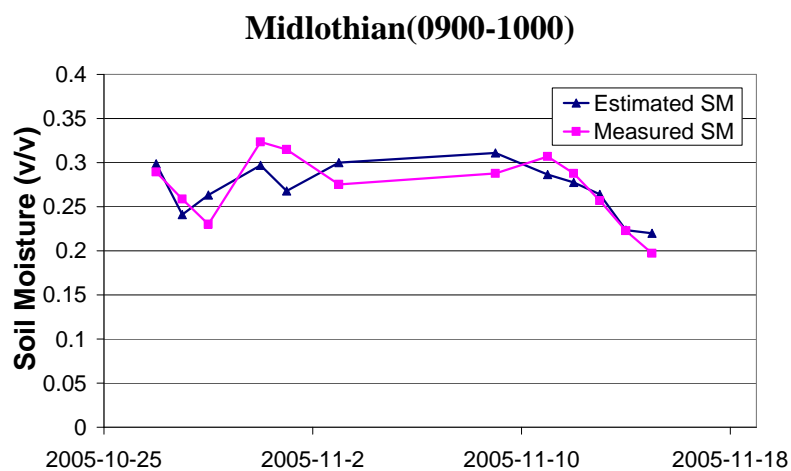


Figure 26: Comparison of estimated soil moisture and recorded soil moisture for Midlothian (0900-1000).

The *Midlothian* (0900-1000) scenario has more abundant data to establish the linear relationship than *Stanley* (1600-1700) scenario as shown in *Figure 25*, which forms a more robust argument for the verification of the linearity. In addition to the data abundance, *Figure 6c* proves the similarity between the soil moisture measurements of 1km and of 300m away from TIR station, which

suggests a high degree of representativeness of the soil moisture data (1km) to the TIR station.

As mentioned in previous sections, the selections of the absolute thresholds for $r^2 > 0.5$ and $RMSE < 3\%v/v$ are totally arbitrary. If not taking these thresholds into account, it is observed that the Midlothian (1000-1100) scenario also has a relatively high degrees of linearity ($r^2 = 0.3923$) and low RMSE ($RMSE = 2.7\%$), and this scenario is just one hourly after the current optimum scenario. Therefore, it can be concluded that for *Midlothian* site, the morning hourly periods from 0900-1100 possess comparably high linear correlations between SM and T_G , and 0900-1000 is more preferable due to the high degree of linearity and low RMSE.

5.2 Discussion

Two optimum scenarios were identified at *Stanley* (1600-1700) and *Midlothian* (0900-1000), whilst other scenarios either do not possess the linearity or have high RMSE values. Small T_G range for the SM- T_G relationship and the large deviations from the SM bands also constraint the applicability of the relationship. The presence of optimum scenarios proves that the linear relationship can exist for some hourly periods on given canopy covers. However, it should be noted that no other obvious trends were observed in terms of the suitability of hourly periods and the effect of vegetation due to a several limitations in the study:

- No seasonal effect were taken into account provided that length of data is limited to one month;
- Soil moisture measurements were not made at the same location as TIR measurements except for *Stanley*. This is because the NAFE'05 project is not specifically designated for the purpose of this study;
- Classification of days of different cloud conditions utilised the shortwave radiation data at *Stanley* and it was assumed applicable to other three sites. This might be true in identifying cloud days due to the closeness of the study sites, but an exception can be found that it may be cloud free in *Stanley*, but a few scattered clouds at other sites. In this case, a small number of inconsistent T_G value could be appear in the data set.

5.2.1 Illogan and Merriwa Park

None of the scenarios at *Illogan* illustrate any linearity from the data set although no vegetation cover was present in the site which enables the accurate measurement of TIR data. One possibility which led to this outcome may be the inappropriate soil moisture representation for the TIR site, as there was 1km distance between the two sites where SM data and TIR data were taken. The limited number of hand measured soil moisture data in *Figure 6a* showed a certain degree of similarity of soil moisture of 1km and 300m from the TIR site, these four measurements are deemed insufficient to prove that the SM measurement made of 300m from the TIR site is completely representative to SM at the vicinity of the TIR site. A huge change in topography (such as sloping, soil type) within 300m is still likely to lead to a large soil moisture difference regardless of the short areal distance.

Merriwa Park also shows no obvious positive correlation (against the 3 criteria) between soil moisture and surface temperature gradient for all scenarios. However, this outcome was expected for *Merriwa Park* because the station based soil moisture has large variances from the hand measured soil moisture. Therefore the soil moisture data used to verify the linear relationship was not representative enough to the soil moisture at the TIR station. Further, *Merriwa Park* also has the

largest density of vegetation cover, TIR data can hardly penetrate through the canopy to accurately measure the surface temperature of soil.

5.2.2 Midlothian and Stanley

Two optimum scenarios were identified at *Stanley* and *Midlothian* at 1600-1700 and 0900-1000 respectively. Both established relationships give 2.4% root mean square errors in estimating the soil moisture. The r^2 and RMSE values associated with each hourly period at these two sites are shown in *Figure 27* and *Figure 28*.

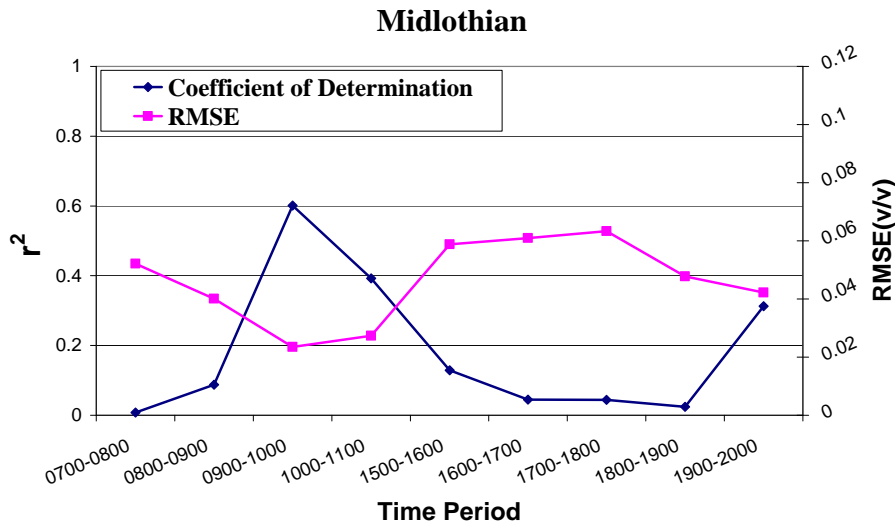


Figure 27: r^2 and RMSE values for all hourly periods at Midlothian

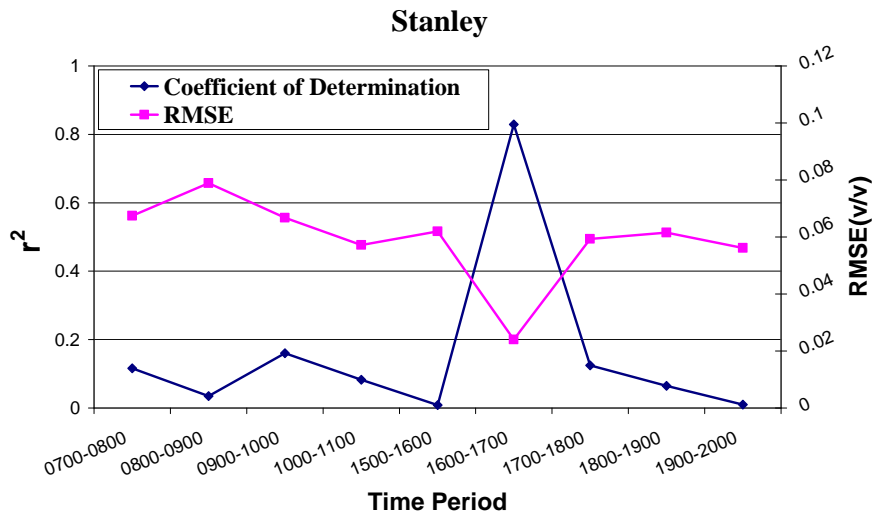


Figure 28: r^2 and RMSE values for all hourly periods at Stanley

It can be seen from *Figure 27*, the correlation (r^2 and RMSE) of the SM- T_G relation increases from the 0700-0800 period and peaks at 0900-1000, followed by a gentle decline of correlation until night time. The preceding and following transitive periods give an evident indication that the morning periods are more superior in describing the linearity than afternoon periods and 0900-1000 is the optimum hourly period among all the morning periods.

At *Stanley* (*Figure 28*), except for the hourly period of 1600-1700, all other periods possess poor linear correlations between soil moisture and surface temperature gradient. A sudden increase of correlation appears at 1600-1700 in the afternoon without any preceding and following transitive

periods that could provide an explainable trend.

Both these scenarios were technically verified to be appropriate for soil moisture retrieval using the thermal infrared data at these two sites during the time where the data was taken. However, the ability of the relationships that can be used for further soil moisture retrieval for other time (e.g. in a year's time) is still doubtful. It is recommended that the two scenario can be tested using the SM and TIR data from NAFE'06 campaign over the same period of time (i.e. November). Thus the accuracy of the estimation could be known by comparing to the field observations. By doing that, new data for NAFE'06 campaign should be able to progressively advance the findings of this study.

5.2.3 Optimum Hourly Period

In discussing the effect of hourly periods, *Illogan* and *Merrwa Park* were excluded because of the non-presence of any satisfactory scenarios. Optimum scenarios occurred at *Stanley* and *Midlothian*, but it is noticed that the optimum hourly periods differ from *Stanley* to *Midlothian*. Afternoon period (1600-1700) is deemed most appropriate to *Stanley* whereas morning period (0900-1000) is regarded more suitable to *Midlothian*.

As mentioned in earlier sections, the morning periods at *Midlothian* could potentially be a preferable hourly periods for T_G computation at *Midlothian*, whereas afternoon hourly period (1600-1700) seems more desirable at *Stanley*. As such, no fixed single hourly periods can be identified as the "best" hourly period for the linear relationship based on the findings of this study. As all these four sites are conditioned by varied topography, canopy cover and soil characteristics, it is more likely that flexible optimum hourly periods would exist depending on these local conditions. Besides, an unverified factor: the latitude of the site, may also affect the best hourly period because different places may have different solar radiation cycle depending on the latitude, which might in turn impact on the surface temperature gradient.

5.2.4 Canopy Effect

Canopy was thought to have great impact on the SM- T_G relationship because it decided how accurate the TIR measurement can be made. One of the objectives of this study was to explore the canopy effect on the relationship from the four study sites. However, the analysis did not discover any clear relationship among the four study sites (with different vegetation cover) regarding canopy effect.

Besides, the information regarding vegetation conditions at each site were not sufficient to aid the canopy analysis. It is likely that in growing season, the density of vegetation could vary greatly in one month's time so that the TIR measurements can be affected. Also, withered leaves of vegetation behave differently from green leaves, in which the green cover evapotranspiration could slower the change of temperature due to the presence of chlorophyll (Nemani *et al.*, 1993). Therefore, a comprehensive study of the canopy effect on the presumed relationship requires sufficient information about the vegetation states. This study failed to fulfill this objective and no conclusions could be drawn regarding the canopy effect.

6. Conclusion and Recommendation

This study was devoted to testing the linear relationship between soil moisture and its surface temperature gradient (obtained from TIR measurements). It was expected that with the aid of the available data at four study sites with different vegetation cover, the best hourly period to be used to compute the temperature gradient could be found and canopy effect on the relationship evaluated.

Available data includes the month-long soil moisture and thermal infrared measurements were obtained from the NAFE'05 campaign. It is noted that except for *Stanley*, the soil moisture and thermal infrared data were taken separately at different ground stations at the distance of 1 kilometre for *Illogan*, *Midlothian* and *Merriwa Park*. A limited number of hand measured soil moisture data taken at a closer distance to the TIR station was therefore utilised to test the representativeness of the soil moisture at the TIR station. The results shows that the soil moisture data used for *Merriwa Park* was least representative to the actual soil moisture at the TIR station, whilst station based SM data at *Midlothian* illustrated a high degree of representativeness of the soil moisture at its corresponding TIR stations. Due to the scarcity of the hand measurements made in *Illogan*, representativeness of the soil moisture data was difficult to determine.

A classification system was developed to eliminate the cloud effect on temperature gradient computation using the shortwave radiation data. Only data on cloud free days was retained for the further use. Hourly periods around the mid-day that may incur inconsistent temperature gradient were also excluded. Nine hourly periods were retained for evaluation purpose. In total, together with the four vegetation cover, 36 scenarios were formed for evaluation.

Three criteria were proposed to test the suitability of linear relation for each scenario: 1. wide temperature gradient range 2. high degree of linearity ($r^2 > 0.5$) and 3. least RMSE ($< 3\% v/v$). The first criteria is based on the fact that a larger T_G range could potentially reduce the sensitivity of T_G on soil moisture estimation, so that it avoids a small uncertainty in T_G to produce a large soil moisture estimation error. The second and the third criterion were based on statistical means to analyse the linearity of the relationship, they were utilised to ensure the maximum degree of linearity whilst producing the least estimating errors.

The analysis for all scenarios revealed two optimum scenarios as shown in *Table 9*. There is no optimum scenario found at *Illogan* and *Merriwa Park*. Possible reason is that the soil moisture was not representative to their corresponding TIR sites.

Table 9: Optimum scenarios for the linear relationship

Site	Hourly period	T_G Range	r^2	RMSE(v/v)
Stanley	1600-1700	0.0756	0.8288	2.4%
Midlothian	0900-1000	0.0637	0.6014	2.4%

The presence of optimum scenarios proves that the linear relationship can exist for some hourly periods on given canopy covers to a certain extent. However, as the results of the analysis do not suggests a perfect linear trend, this study does not deny the possibility of other relationship (i.e. logarithm or exponential) between the Soil Moisture and Surface Temperature Gradient.

Based on the findings of the study, instead of one fixed optimum hourly period, the optimum hourly period to be used in the relationship could be flexible. Both morning and afternoon periods possess the ability to best describe the SM- T_G relation, and the selection of best hourly period may be

ultimately depending on the canopy cover, soil characteristics, topography and the latitude of the earth. However, the influence of factors still needs to be verified by more investigation and study.

Although canopy effect was proved to impact on the thermal infrared measurement by other researchers, the analysis results of this study did not discover any clear relationship among the four study sites regarding the canopy effect. Hence, the no conclusion can be drawn regarding the canopy effect based on the results of this study.

It is recognised that the a number of limitations were present in this research, such as the month-long data set did not enable the consideration of seasonality and certain weaknesses existed in the cloud classification system by solely using the shortwave radiation data at *Stanley*. The largest uncertainty in this study is the compatibility of soil moisture and thermal infrared data as they were not made at exactly the same locations. Even the hand measurements provided to test the soil moisture had 300m distance away from the TIR sites.

Although the data and the analysis in this research produced encouraging results – proved the suitability of the use of linear relationship for some hourly periods on given canopy covers but the results of analysis is not sufficient to give full explanations on the canopy effect. Further studies are needed in order to enable the application of the SM- T_G relationship:

1. The two optimum scenarios proposed by this study can be verified using the SM and TIR data from future NAFE'06 campaign over the same period of time (i.e. November).
2. It is recommended that soil moisture and thermal infrared data should be taken at the same location for each study site, this enables the largest extent of representativeness of soil moisture at the TIR site.
3. Provided the soil moisture and thermal infrared data were made at same location, a prolonged data taking time is encourage in order to cover the extreme soil moisture contents and account for the seasonality of the relationship.
4. Sufficient information about the vegetation conditions and states are required for a comprehensive study of the canopy effect on the presumed relationship.
5. Develop a more systematic method for cloud classification.

7. References

- Alexandrov, V. A., and Hoogenboom, G., (2000). The impact of climate variability and change on crop yield in Bulgaria. *Agricultural and Forest Meteorology*, 104, 315–327.
- Ben-asher, J., Matthias, A.D. and Warrick, A.W., (1983). Assessment of evaporation from bare soil by infrared thermometry. *Soil Science Society of American Journal*, 47, pp. 185–191.
- Betts, A. K., Ball, J. H., Baljaars, A. C. M., Miller, M. J., and Viterbo, P., (1994). Coupling Between Land-Surface, Boundary-Layer Parameterizations and Rainfall on Local and Regional Scales: Lessons from the Wet Summer of 1993. *Fifth Conf. on Global Change Studies: American Meteor. Soc.*, Nashville, 174 -181.
- Choudhury, B. J., Schmugge, T. J., Chang, A., and Newton, R. W., (1979). Effect of Surface Roughness on the Microwave Emission from Soils. *J. of Geophysical Res.*, 84(C9): 5699-5706.
- Curran, P. J., (1985). *Principles of Remote Sensing*. Longman Scientific and Technical, UK, 282pp.
- Curran, P.J., Foody, G.M., Kondratyev K.Ya., Kozoderov, V.V. and Fedchenko, P.P., (1990) Remote sensing of soils and vegetation in the USSR. London ; New York : Taylor & Francis, c1990.
- Dobson, M. C., Ulaby, F. T., Hallikainen, M. T., and El-Rayes, M. A., (1985). Microwave Dielectric Behaviour of Wet Soil - Part II: Dielectric Mixing Models. *IEEE Trans. Geosci. Rem. Sens.*, GE-23(1): 35-46.
- Elachi, CHARLIES (2006) *Introduction to the physics and techniques of remote sensing*. Hoboken, N.J. : Wiley, c2006.
- Engman, E. T., (1991). Application of Microwave Remote Sensing of Soil Moisture for Water Resources and Agriculture. *Rem. Sens. Environ.*, 35: 213-226.
- Engman, E. T., (1992). Soil Moisture Needs in Earth Sciences. In: *Proc. International Geoscience and Remote Sensing Symposium (IGARSS)*, 477-479.
- Engman, E. T., & Chauhan, N. (1997). Status of microwave soil moisture measurements with remote sensing. *Remote Sensing of Environment*, 51, 189– 198.
- Entekhabi, D., Nakamura, H., and Njoku, E. G., 1993. Retrieval of Soil Moisture by Combined Remote Sensing and Modeling. In: Choudhury, B. J., Kerr, Y. H., Njoku, E. G., and Pampaloni, P. (Eds.), *ESA/NASA International Workshop on Passive Microwave Remote Sensing Research Related to Land-Atmosphere Interactions*, St. Lary, France, 485-498
- Fung AK, Li Z, Chen KS. (1992). Backscattering from a randomly rough dielectric surface. *IEEE Transactions on Geoscience and Remote Sensing* 30(2): 356–369.
- Galantowicz, J. F., Entekhabi, D., and Jackson, T. J., (1999). Efficient Models of Soil Heat and Water Flow and Emission for Moisture and Temperature Determination from Remote Sensing Observations. *IEEE Trans. Geosci. Remote Sens.*
- Hendrickx, Jan M. H.; van Dam, Remke L.; Borchers, Brian; Curtis, John O.; Lensen, Henk A.; Harmon, Russell S. (2003) Worldwide distribution of soil dielectric and thermal properties:

Detection and Remediation Technologies for Mines and Minelike Targets VIII. Edited by Harmon, Russell S.; Holloway, John H., Jr.; Broach, J. T. Proceedings of the SPIE, Volume 5089, pp. 1158-1168 (2003).

Idso, S. B., Jackson, R. D., Reginato, R. J., Kimball, B. A., and Nakayama, F. S., (1975). The Dependence of Bare Soil Albedo on Soil Water Content. *Journal of Applied Meteorology*, 14: 109-113.

Fast, J. D., and McCorcle, M. D., 1991. The Effect of Heterogenous Soil Moisture on a Summer Baroclinic Circulation in the Central United States. *Mon. Wea. Rev.*, 119: 2140-2167.

Jackson, T. J., (1997). Soil Moisture Estimation Using Special Satellite Microwave/Imager Satellite Data Over a Grassland Region. *Water Resour. Res.*, 33(6): 1475-1484.

Jackson, T. J., Hawley, M. E., and O'Neill, P. E., (1987). Preplanting Soil Moisture Using Passive Microwave Sensors. *Water Resources Bulletin*, 23(1): 11-19.

Jensen, John R (2006) *Remote sensing of the environment : an earth resource perspective* Upper Saddle River, NJ : Pearson Prentice Hall, c2006.

Jordan, J. D., and Shih, S. F., (1993). Comparison of Thermal-Based Soil Moisture Estimation Techniques on a Histosol. *Soil and Crop Science Society of Florida Proceedings*, 52: 83-90.

Mitra, D. S., & Majumdar, T. J. (2004). Thermal inertia mapping over the Brahmaputra basin, India using NOAA-AVHRR data and its possible geological applications. *International Journal of Remote Sensing*, 225(16), 3245–3260.

Monteith, J.L., (1981), Evaporation and surface temperature. *Quarterly Journal of the Royal Meteorological Society*, 107, pp. 1–27.

Nemani, R., Pierce, L., and Running, S., 1993, Developing satellite-derived estimates of surface moisture status. *Journal of Applied Meteorology*, 32, 548–557.

Njoku, E. G., and Entekhabi, D., (1996). Passive Microwave Remote Sensing of Soil Moisture. *J. Hydrol.*, 184: 101-129.

Oh Y, Sarabandi K, Ulaby FT. (1992). An empirical model and an inversion technique for radar scattering from bare soil surfaces. *IEEE Transactions on Geoscience and Remote Sensing* 30(2): 370–381.

Oh Y, Sarabandi K, Ulaby FT. (1994). An inversion algorithm for retrieving soil moisture and surface roughness from polarimetric radar observation. In *Proceedings, International Geoscience and Remote Sensing Symposium (IGARSS)*, Pasadena; 1582–1584.

Ottli, C., and Vida-Madjar, D., (1994). Assimilation of Soil Moisture Inferred from Infrared Remote Sensing in a Hydrological Model Over the HAPEX-MOBILHY Region. *J. Hydrol.*, 158: 241-264.

Pegram G.G.S.,(2006). Soil Moisture From Satellites: Daily Maps Over RSA, WRC Report No. K5/1683. South Africa, 20006

Peplinski, N. R., Ulaby, F. T., and Dobson, M. C., (1995). Dielectric Properties of Soils in the 0.3-1.3 GHz Range. *IEEE Trans. Geosci. Rem. Sens.*, 33(3): 803-807.

- Pratt, D. A. & Ellyett, C. D. (1979). The thermal inertia approach to mapping of soil moisture and geology. *Remote Sensing of Environment*, 8, 151-168.
- Price, J.C., (1980), The potential of remotely sensed thermal infrared data to infer surface soil moisture and evaporation. *Water Resources Research*, 16, pp. 787–795.
- Reginato, R.J., Idso, S.B., Vedder, J.F., Jackson, R.D., Blanchard, M.B. and Goettelman, R., (1976), Soil water content and evaporation by thermal parameters obtained from ground-based and remote measurements. *Journal of Geophysical Research*, 81, pp. 1617–1620.
- Sadeghi, A. M., Hancock, G. D., Waite, W. P., Scott, H. D., and Rand, J. A., (1984). Microwave Measurements of Moisture Distributions in the Upper Soil Profile. *Water Resour. Res.*, 20(7): 927-934.
- SASMAS (2003) Scaling and Assimilation of Soil Moisture And Streamflow Project. Retrieved on 31/08/2006 <http://www.civenv.unimelb.edu.au/~jwalker/data/sasmas/index.htm>
- Scott, C. A., Bastiaanssen, W. G. M., & Ahmad, M. U. D. (2003). Mapping root zone soil moisture using remotely sensed optical imagery. *Journal of Irrigation and Drainage Engineering-Asce*, 129, 326-335.
- Shepherd, A., McGinn, S. M., and Wyseure, G. C. L., (2002). Simulation of the effect of water shortage on the yields of winter wheat in North-East England. *Ecological Modelling*, 147, 41–52.
- Sobrino, J. A., & El Kharraz, M. H. (1999). Combining afternoon and morning NOAA satellites for thermal inertia estimation 2. Methodology and application. *Journal of Geophysical Research*, 104(D8), 9455–9465.
- Su, Z., Troch, P. A., de Troch, F. P., Nochtergale, L., and Cosyn, B., 1995. Preliminary Results of Soil Moisture Retrieval From ESAR (EMAC 94) and ERS-1/SAR, Part II: Soil Moisture Retrieval. In: de Troch, F. P., Troch, P. A., Su, Z., and Cosyn, B. (Eds.), *Proceedings of the second workshop on hydrological and microwave scattering modelling for spatial and temporal soil moisture mapping from ERS-1 and JERS-1 SAR data and macroscale hydrologic modelling (EV5V-CT94-0446)*. Institute National de la Recherche Agronomique, Unité de Science du Sol et de Bioclimatologie, France, 7-19.
- Tramutoli, V., Claps, P., Marella, M., Pergola, N., & Sileo, C. (2000). Feasibility of hydrological application of thermal inertia from remote sensing. 2nd Plinius Conference on Mediterranean Storms, Siena, Italy, 16–18 October 2000.
- Troch, P. A., Vandersteene, F., Su, Z., Hoeben, R., and Wuethrich, M., (1996). Estimating Microwave Observation Depth in Bare Soil Through Multi-Frequency Scatterometry. In: *Proc. Of the First EMSL User Workshop, SAI, JRC, Ispra, Italy*.
- Ulaby, F.T., P.C. Dubois and J. Van Zyl. (1996). Radar mapping of surface soil moisture. *J. Hydrol.* (Amsterdam) 184:57-84.
- Van de Griend, A. A., and Engman, E. T., 1985. Partial Area Hydrology and Remote Sensing. *J. Hydrol.*, 81: 211-251.
- Verstraeten, W. W., Veroustraete, F., van der Sande, C. J., Grootaers, I., & Feyen, J. (2006). Soil Moisture Retrieval Using Thermal Inertia, Determined with Visible and Thermal Spaceborne Data,

Validated for European Forests. *Remote Sensing of Environment*, 101, 299-314.

Vicente, S., Pons, F. n., & Cuadrat, P. (2004). Mapping soil moisture in the central Ebro river valley (northeast Spain) with Landsat and NOAA satellite imagery: a comparison with meteorological data. *International Journal of Remote Sensing*, 25, 4325-4350.

Walker, J. P. (1999) Estimating Soil Moisture Profile Dynamics From Near-Surface Soil Moisture Measurements and Standard Meteorological Data. *Doctor of Philosophy in Environmental Engineering Thesis* submission to The University of Newcastle, 1999

Walker, J. P., Houser, P. R. and Willgoose, G. R., (2004a). Active Microwave Remote Sensing for Soil Moisture Measurement: A Field Evaluation Using ERS-2. *Hydrological Processes*, 18:1975-1997. doi:10.1002/hyp.1343

Walker, J. P. and Houser, P. R. (2004b). Requirements of a Global Near-Surface Soil Moisture Satellite Mission: Accuracy, Repeat Time, and Spatial Resolution. *Advances in Water Resources*, 27:785-801. doi:10.1016/j.advwatres.2004.05.006.

Wang, J. R., and Schmugge, T. J., (1980). An Empirical Model for the Complex Dielectric Permittivity of Soils as a Function of Water Content. *IEEE Trans. Geosci. Rem. Sens.*, GE-18(4): 288-295.

Western, A. W., Green, T. R., and Grayson, R. B., (1997). Hydrological Modelling of the Tarrawarra Catchment; Use of Soil Moisture Patterns. In: McDonald, A. D., and McAleer, M. (Eds.), *Proc. MODSIM 97 International Congress on Modelling and Simulation*, Hobart, Australia, 409-416.

Wood, E. F. (1997). Effects of soil moisture aggregation on surface evaporative fluxes. *Journal of Hydrology*, 190, 397-412.

Woodhouse, Iain H. (2005) *Introduction to microwave remote sensing* Boca Raton, FL : Taylor&Francis, 2005.

Xue, Y., & Cracknell, A. P. (1995). Advanced thermal modeling. *International Journal of Remote Sensing*, 16, 431-446.